2012-01-01

Design and Development of an Optically Accessible High Pressure Combustor

Jesus Nunez
University of Texas at El Paso, jnunez4@miners.utep.edu

DESIGN AND DEVELOPMENT OF AN OPTICALLY ACCESSIBLE HIGH PRESSURE COMBUSTOR

JESUS NUNEZ MICHEL

Mechanical Engineering Department

APPROVED:

Norman Love, Ph. D., Chair

Ahsan Choudhuri, Ph.D.

Jose F. Espiritu, Ph.D.

Benjamin C. Flores, Ph.D.
Interim Dean of the Graduate School

DESIGN AND DEVELOPMENT OF AN OPTICALLY ACCESSIBLE HIGH PRESSURE COMBUSTOR

by

JESUS NUNEZ MICHEL

THESIS

Presented to the Faculty of the Graduate School of

The University of Texas at El Paso

in Partial Fulfillment

of the Requirements

for the Degree of

MASTER OF SCIENCE

Department of Mechanical Engineering

THE UNIVERSITY OF TEXAS AT EL PASO

May 2012

Acknowledgments

I would like to acknowledge my advisor and mentor Dr. Norma Love for providing me with the opportunity and encouragement to follow my academic pursuits. Dr. Ahsan Choudhuri, CSERT Lab, and Loya Innovation Fund for providing the funding and opportunity to conduct this research. Also would like to acknowledge my lab coworkers Sudipa Sarker and Carlos Valdez.

Abstract

Currently in the US there is a push to reduce the nation's energy dependence from foreign fuel sources. One of the most abundant fuels in the US is coal with the nation's coal reserve accounting for 25% of the coal in the world. Due to coal being an abundant resource in the US and the need to reduce the dependency on foreign fuel sources coal derived synthetic fuels have been studied for use in gas turbines. Modern gas turbine combustors must operate over a range of different fuel compositions which includes fuels with high hydrogen fuel content (HHC). To ensure the implementation of HHC in power generation without negotiating operational or emission advantages, a study of the flame stability regime and behavior of HHC under realistic gas turbine condition is needed. Thus this thesis presents the development of an optically accessible high-pressure turbine combustor. The design parameters of the combustor developed are based on a 500 kW power and 1.5 MPa pressure which is representative of an actual gas turbine. Furthermore, the combustor has the flexibility of operating with variable syngas compositions along with a variety of fuel to analyze the flame structure, flow field characterization using high speed particle image velocimetry (PIV), and flashback propensity in high hydrogen content fuel under realistic gas turbine condition. The combustor has been built and tested and is available for use for testing of a variety of fuels.

Table of Content

List of Tables

List of Figures

Nomenclature/List of Symbols

A= Area
A_e=Exhaust Area
A_T =Throat Area
$\propto_j$=Coefficient of Thermal Expansion of Joint Material
$\propto_b$=Coefficient of Thermal Expansion of Bolt
C_p=Specific Heat at Constant Pressure per Unit Mass
d = Diameter of bolt
F_t = Thermal load
F_p = Preload
f=fuel-air ratio
g=gravity constant
h = Heat transfer coefficient
h_A= Total Head Loss
h_L=Minor Head Loss
K_b= Coefficient Of Friction Bolt
k_b = Stiffness of bolt
k_j = Stiffness of joint
L_b=Length of Bolt
$\dot{m}$=Mass flow rate
m_a=airflow rate
Ma=Mach number
P=Pressure
P_a=Ambient Pressure
P_C=Chamber pressure
P_e=Exhaust Pressure
R=Universal gas constant
R_{total} = Total thermal resistance
Q =Production of heat
T=Temperature
T_{Ad}=Adiabatic Flame temperature
T_b= Initial torque
T_C=Chamber temperature
T_∞=Free Stream Temperature
u=Velocity
u_e=Exhaust Velocity
v=Velocity
γ=Specific heat constant

1. Introduction

1.1 INTRODUCTION

Currently in the US there is a push to reduce the nation's energy dependence from foreign countries. One of the most abundant fuels in the US is coal with the nation's coal reserve accounting for 25% of the coal in the world [US DOE 2011]. Coal is primarily used for electric power production and currently produces more than half the electricity produced in the US [US DOE 2011]. Due to coal being an abundant resource in the US and the need to reduce the dependency on foreign fuel sources coal derived synthetic fuels have been studied for use in gas turbines. Gas turbines have been used for power generation since 1939 and were first explored by the Brown Bovery Company located in Neuchâtel, Switzerland [ASME 1988]. Current application for gas turbines include the gas and oil industry, emergency power generation facilities, independent power production, and a number of other industrial applications [EPA 2000].

A gas turbine is an internal combustion engine operating with rotary motion. The main components of the engine are the compressor, the combustor, and the turbine. In the compressor section air is drawn in and compressed where it is then directed to the combustion chamber where fuel is added, ignited, and burned. The hot gases produced are then routed to the turbine section where energy from the exhaust gas is recovered in the form of shaft power. More than 50 % of the power produced is then routed to supply the motion of the compressor, while the rest is available to drive and external load [EPA 2000]. The exiting heat content from the exhaust gas is then discarded with the following applications: without heat recovery in an open cycle, recovered with heat exchangers, and can be used to preheat the air entering the compressor in a

regenerating cycle, or recovered to produce steam used in a steam turbine for power production in a Rankine cycle [EPA 2000]. Typical Brayton Cycle thermal efficiencies range from 15-42 percent [EPA 2000].

Synthetic fuels have the capability to produce lower pollutant emission compared to traditional coal derived power sources. Due to the use of alternative types of fuels such as synthetic gas, modern turbine combustors will be required to operate over a range of different fuel compositions which includes fuels with high hydrogen fuels content. Hydrogen a common component of a syngas fuel mixture cause high laminar flame speed, changes the range of flammability limits, and increases the propensity of a flame to flashback [Daniele et al. (2010)]. Flashback is defined as the point when the flame propagates upstream of the region where it is intended to affix. Flashback may occur due to propagation in the core flow, propagation in the boundary layer, propagation due to combustion induced vortex breakdown, and propagation due to combustion instabilities [Tse and Zhu 2004]. Due to the use of these newly developed fuels the need to study flame characteristics under particularly realistic turbine conditions is needed.

1.2 OBJECTIVE

The main objective of this thesis is to detail the design of an optically accessible high pressure combustor which can operate with a variety of fuels. This thesis will cover many design aspects of the high pressure combustor test section which will incorporate the use of a cooling system, fittings, and test facilities. Also included is the heat transfer analysis: FEA, CAD modeling, manufacturing, part assembly, current status of the testing facility, and future work needed.

1.3 DESIGN PARAMETERS AND CONFIGURATION

The combustor is designed to operate up to 1.5 MPa and temperatures reaching up to 2400K. This temperature and pressure is selected due to the high hydrogen fuel composition that will be used in testing as well as pressure representative of an actual gas turbine. The air mass flow rate is designed to be a maximum of 81.93 g/s and will be provided by a continuous compressed air supply. The fuel used will be (H_2-CO) with a maximum flow rate of 35.77 g/s, with hydrogen being varied up to 30 percent of the fuel composition.

The combustor is composed of four primary modular sections including an inlet static mixer, an inlet cap, an optically accessible combustion chamber, and a variable exhaust throat area restrictor composed of a converging nozzle and exhaust. The combustor will incorporate a cooling system in the inner and outer section of the combustor. The combustion chamber will also be operable while accommodating a configurable quartz burner to help show how the burner geometry can affect flashback and the use of instrumentation ports to measure pollutant emissions. The CAD model of the combustor can be seen below in Figure (1)

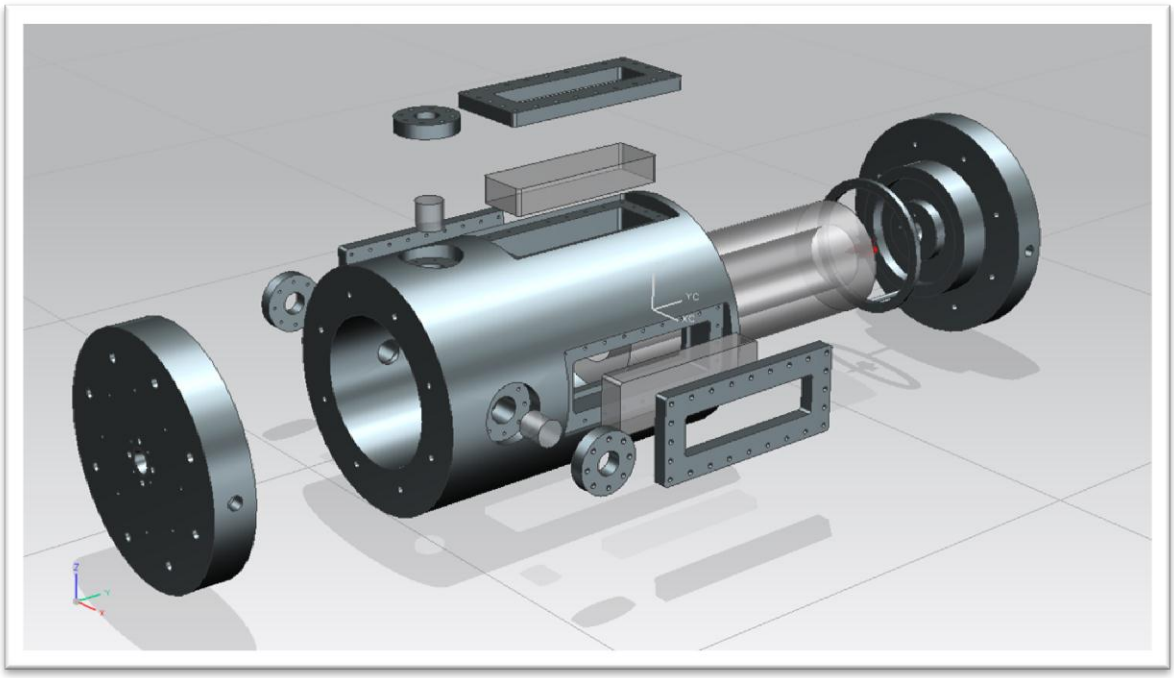

Figure 1 CAD Model High Pressure Combustor

1.4 THESIS ORGANIZATION

Chapter 1 provides the main objective and a brief description of the design configuration and the operating parameters of the combustor.

Chapter 2 provides a summary of current operational combustors operating at comparable conditions and used for similar research..

Chapter 3 will cover heat transfer calculations and FEA of the components. Also included will be the cooling flow needed.

Chapter 4 will cover the design configuration of the combustor, dimensions, bolt calculation, as well as the stand for the test facility, manufacturability, and assembly.

Chapter 5 will cover the results of the test facility and future work needed.

2. Background and Literature Review

As a starting point in the design and development of the high pressure combustor presented in this thesis it was necessary to investigate previous design and tested combustors operating under similar conditions. This chapter will review some of these combustors in operation and discuss the similarities and differences between this current design and those previously developed. Also included will be the current operation ambient combustor being used at the University of Texas at El Paso (UTEP) and the influence it had on the development of the current design.

2.1 UTEP AMBIENT COMBUSTOR

Currently at UTEP there is an operational optically accessible combustor operating under ambient conditions. The design is of importance due to the correlation and design parameters taken from the previous design and used in the current design. The main area of research the ambient combustor has been used for pertains to flashback properties in syngas fuels. Various test and journal publications have been published (Bidhan et. al 2011), using the ambient combustor as a test facility, pertaining to that study.

Different fuel mixtures have been used in the combustor including $H_2 - CO$ and $H_2 - CH_4$ mixtures. The combustor rig is shown in Figure (2) and is set up using four configurable models: the inlet manifold, static mixer, swirler burner with quartz tube, and the combustion chamber. The quartz windows located on the main combustion section allow for high speed imaging of flashback characteristics. The inner dimensions for the combustor is 130 millimeters similar to the high pressure combustor as well as the fuel and air inlet manifold design and static mixer.

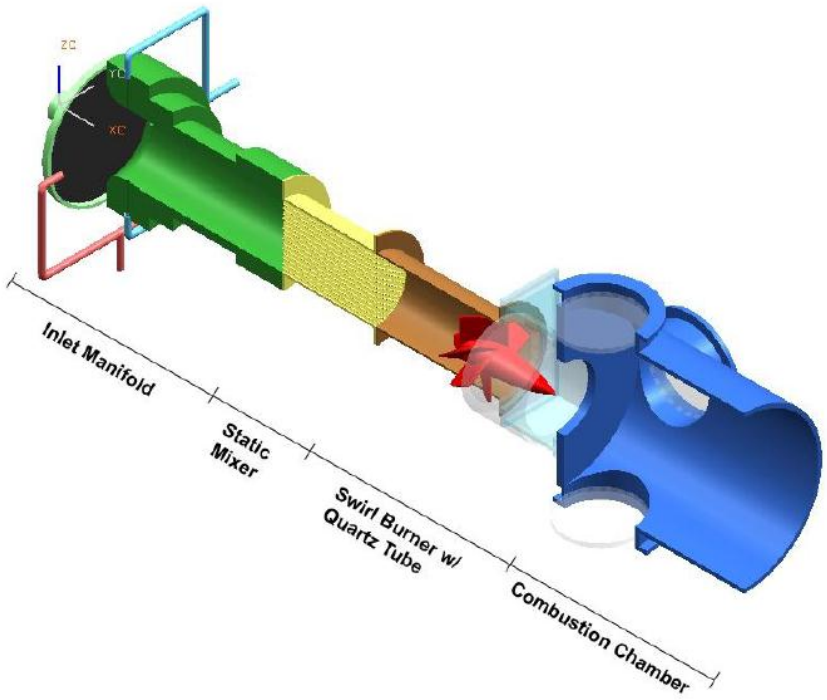

Figure 2 UTEP Ambient Combustor

2.2 HIGH PRESSURE COMBUSTORS

There are currently a number of different combustors being used for related experiments and using similar operating conditions. These combustor designs were reviewed and taken into consideration with the current design. A brief description and operating conditions are listed below.

In Cambridge University High Pressure Combustion Lab a combustor was design to operate up to 600 °C and 1 MPa with an air mass flow rate of .9 kg/s. The use of an optical section with 120x130 mm^2 windows were used and combustion takes place in a 130 mm diameter quartz tube, the same dimensions and materials as our current design. The Cambridge combustor also

implements a cooling system with air flowing between the inside quartz chamber and outer chamber and was used as a starting reference point for the cooling system of the current combustor developed. The pressure drop in the combustor is controlled using a variable area flow restrictor in the exit nozzle similar to our current design (Cambridge 2009).

The University of California Irvine Combustion Laboratory (UCICL) has two operational testing combustors. One used for high pressure combustion experiments with optical access, the second used for long duration experiments. The flow rate reaching 1 kg/s and pressure up to 15 bar (Irvin 2011).

The National Energy Technology Laboratory (NETL) has two operational high-pressure combustor facilities. A dynamic gas turbine with optical access and operating pressures of up to 10 bar and air flow at .75 kg/s while using natural gas and liquid fuels. The second combustion facility is used for computational fluid dynamic testing and modeling of combustion. The combustor has optical access and can operate with variable fuel and pressures up to 22 bar (National Energy Technology Laboratory)

Pennsylvania State University's High Pressure Combustion Lab performs test in the area of solid-fuel formulation, development, and propulsive performance. The use of a high Solid Propellant Strand Burner (SPSB) with pressure in the chambers reaching up to 655 bar with optical access used to investigate the flame spreading process. Also in use is an "Ultra High Pressure Strand Burner" with pressures up to 2068 bar (PSU 2011).

Physical Science Inc. has developed an optically accessible combustor for planar laser induced fluorescence measurements. The combustor utilizes commercial styled gas-turbine fuel injectors and has the capability of operating at pressures up to 50 bars. Current work has been limited to

operating at 20 bars with a maximum flow rate of 0.4 kg/s. The inlet air is preheated to a temperature ranging from 400 K to 550 K before combustion. The combustor design consists of four main components: a pressure vessel with inlet and exhaust flanges, fuel injection support and linear system, water cooled exhaust orifice, and a water cooled exhaust test section. The combustion gases are contained using a ceramic liner that protects the chamber from the heat load of the flame. The region between the liner and outer pressure vessel is purged with nitrogen flow. As the exhaust gas exists the chamber, it is water cooled in the exhaust section (J.H. Frank, M. F. Miller, M G. Allen)

A high-pressure design was also designed in Italy using natural gas and hydrogen as the fuel source. The combustor is rated at 10 bars and can operate under duel fuel operation (liquid and gaseous). An axial swirler device is used operating with 8 holes for fuel injection. The combustor is air-cooled and utilizes 800 louvers to cool down the chamber wall. The flame is stabilized using a combination of a swirler as well as recirculation of air. The test rig consists of an alloy steel pressure vessel, designed in modular form, utilizing a lamination valve at the exit to control the pressure in the combustor. The combustor metal temperature, air flow, and burner exit temperatures are recorded using thermocouples with an operating range of 400 to 1200 °C. The use of pressure taps is also implemented to monitor pressure drops and high frequency response pressure transducers to measure pressure fluctuation (Tomezak, et al)

Sato study involved a high pressure combustor with a cylindrical section of 500mm and a length up to 600 mm for combustion. The use a removable electric heater is used for ignition. The combustor has optical access with nine windows on the chamber walls. The pressure rating of the chamber reaching up to 200 bar and temperatures reaching up to 900 K. Fuel is sprayed with the use of a high pressure pump and injected into the accumulator (Konishi et al., 1988).

3. Design Methodology

3.1 ADIABATIC FLAME TEMPERATURE

The first step in the design of the combustor was to calculate the adiabatic flame temperature of combustion. The use of the software STANJAN was used to calculate the adiabatic temperature. The values used for calculation can be found in Appendix A. The fuels used were a mixture of carbon monoxide (CO), hydrogen (H_2), and air. The balanced equation for a 70% CO 30% H_2 fuel mixture is presented below.

$$0.7\ CO + 0.3H_2 + 0.5(O_2 + 3.76\ N_2) -> 0.7CO_2 + .03\ H_2O + 1.88\ N_2$$

The adiabatic flame temperature using STANJAN was found to be 2400 K. This was set as a parameter for the temperature which the combustor would be theoretically subjected to.

3.2 WALL TEMPERATURE

After finding the adiabatic flame temperature it was then needed to find the inner wall temperature of the combustor in relation to time. Due to the combustor being composed of modular sections and operable under different configurations it was necessary to find the wall temperature for both stainless steel and quartz materials. Equation (1) and Equation (2) was then used to solve for the inner quartz and stainless steel wall temperature as a function of time. The temperature plot for the quartz stainless steel wall can be seen in Figure (3) and Figure (4) respectively and Table (1) list the properties used.

$$\dot{Q} = \dot{m}C_p\frac{dT}{dx} = hA(T_{Ad} - T) \quad (1)$$

$$T = T_{Ad} + (T_\infty - T_{Ad})e^{\left(-\frac{Aht}{C_p\dot{m}}\right)} \quad (2)$$

Table 1 Equation 1 and 2 Properties

T_{Ad}	**2400 K**
T_{∞}	298 K
$A_{stainles}$	$.63\ m^2$
A_{quartz}	$.28\ m^2$
$h_{stainless}$	$25\ W/(m^2\ K)$
h_{quartz}	$26\ W/(m^2\ K)$
C_p	$1.34\ J/g\ K$
$\dot{m}$	35 g/s

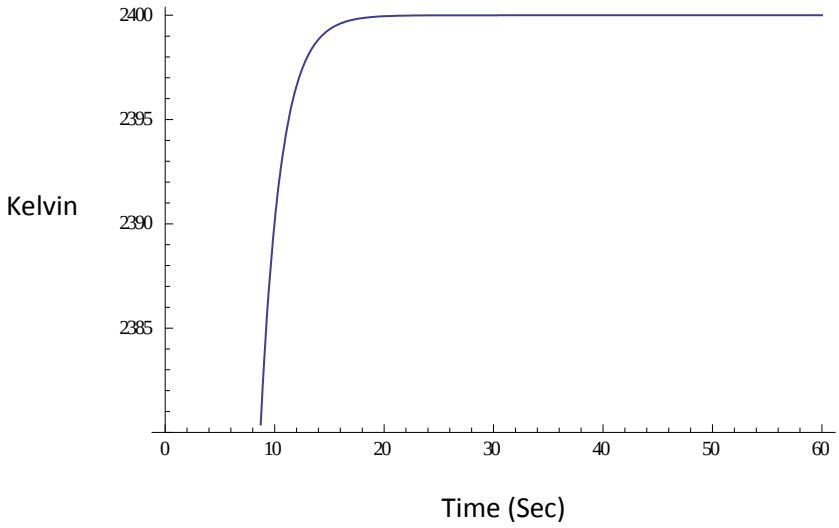

Figure 3 Stainless Steel Wall Temperature as a Function of Time

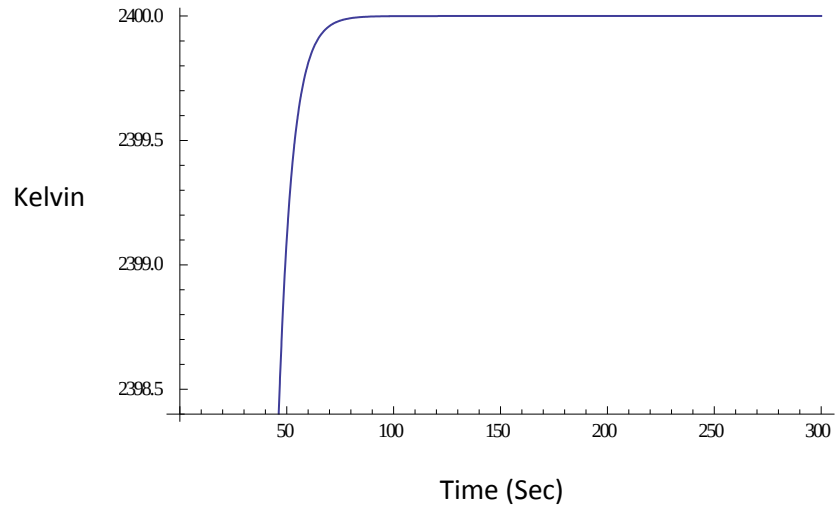

Figure 4 Quartz Temperature as a Function of Time

3.3 FINITE ELEMENT ANALYSIS

Once the adiabatic flame temperature and the initial wall temperature was calculated it was then necessary to use finite element analysis to find the safe operational conditions and dimensions of the combustor. The use of the program UGS NX and NX Nastran was used to conduct the analysis.

3.3.1 Quartz Tube

The first analysis conducted was on the quartz tube. The thickness of the quartz was found by iterating the wall temperatures and thickness of the quartz tube using NX Nastran Design Simulation until an operating temperature of 1100K and a wall thickness of 58 mm was found to give an acceptable result. For the design simulation a fixed constraint was placed in the end of the quartz tube limiting the movement of the six degrees of freedom representing the actual constrain on the ends of the quartz tube occurring due to the end cap and front cap restricting pockets. A temperature load of 1100 K was used representing the wall temperature simultaneously with a pressure load inside the tube of 1.5 MPa. A 10 node tetrahedral mesh was used with an overall element size of 0.0127 meters. This size mesh was checked by performing

multiple iterations with decreasing element size and was found to converge on the given results with changes being minimal. The quartz properties in the finite element analysis can be found in Table (2) while the FEA results in Figure (5) and Figure (6) show the displacement and stress analysis of the quartz tube. The maximum stress results where 43.11 MPa while the maximum tensile stress of 50 MPa is given for the fused quartz material. A maximum displacement of 0.005969 millimeters occurs in the mid section of the quartz tube. Deformations are set at a factor of 10 to show displacement location.

Table 2 Fused Quartz Properties (Heraeus 2009)

Technical properties

	TSC-3®	TSC-4	TSC-Synthetic
Mechanical Data			
Density (g/cm³)	2.2	2.2	2.2
Mohs Hardness	5.5 ... 6.5	5.5 ... 6.5	5.5 ... 6.5
Micro Hardness (N/mm²)	8600 ... 9800	8600 ... 9800	8600 ... 9800
Knoop Hardness (N/mm²)	5800 ... 6100	5800 ... 6100	5800 ... 6100
Modulus of elasticity at 20°C (N/mm²)	7.3×10^4	7.3×10^4	7.3×10^4
Modulus of torsion (N/mm²)	3.0×10^4	3.0×10^4	3.0×10^4
Poisson's ratio	0.16	0.16	0.16
Compressive strength (approx.) (N/mm²)	1110	1110	1110
Tensile strength (approx.) (N/mm²)	50	50	50
Bending strength (approx.) (N/mm²)	65	65	65
Torsional strength (approx.) (N/mm²)	30	30	30
Sound velocity (m/s)	5700	5700	5700
Thermal Data			
Softening temperature (°C)	1730	1730	1730
Annealing temperature (°C)	1200	1200	1200
Strain temperature (°C)	1080	1080	1080
Max. working temperature continuous (°C)	1050	1050	1050
short-term (°C)	1350	1350	1350

	TSC-3®	TSC-4	TSC-Synthetic
Mean specific heat (J/kg*K)			
0 ... 100°C	772	772	772
0 ... 500°C	964	964	964
0 ... 900°C	1052	1052	1052
Heat conductivity (W/m*K)			
20°C	1.38	1.38	1.38
100°C	1.47	1.47	1.47
200°C	1.55	1.55	1.55
300°C	1.67	1.67	1.67
400°C	1.84	1.84	1.84
950°C	2.68	2.68	2.68
Mean expansion coefficient (K^{-1})			
0 ... 100°C	5.1×10^{-7}	5.1×10^{-7}	5.1×10^{-7}
0 ... 200°C	5.8×10^{-7}	5.8×10^{-7}	5.8×10^{-7}
0 ... 300°C	5.9×10^{-7}	5.9×10^{-7}	5.9×10^{-7}
0 ... 600°C	5.4×10^{-7}	5.4×10^{-7}	5.4×10^{-7}
0 ... 900°C	4.8×10^{-7}	4.8×10^{-7}	4.8×10^{-7}
-50 ... 0°C	2.7×10^{-7}	2.7×10^{-7}	2.7×10^{-7}

Electric Data

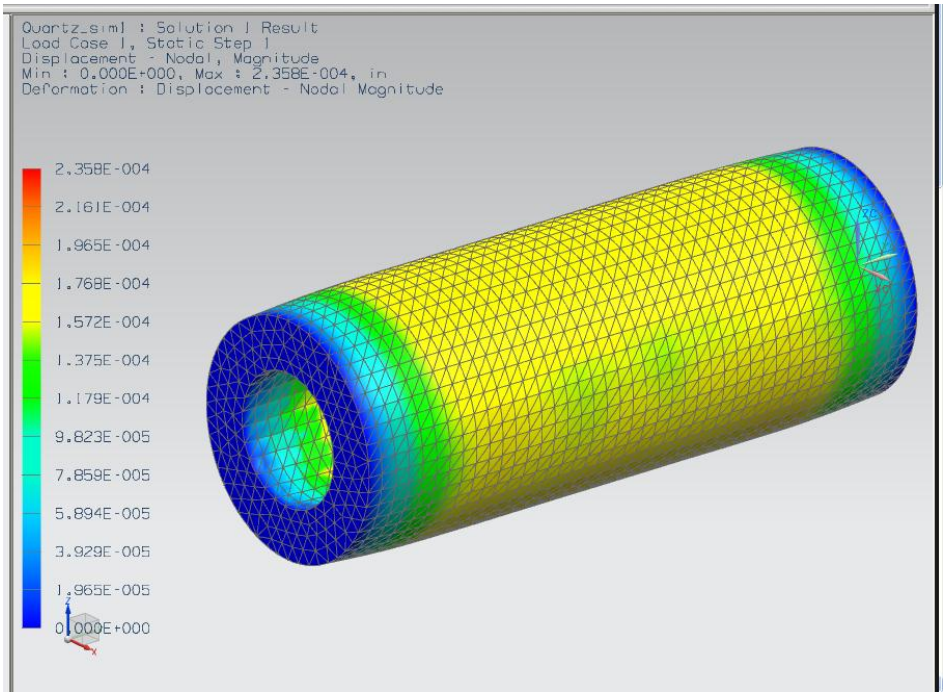

Figure 5 Quartz Tube Displacement

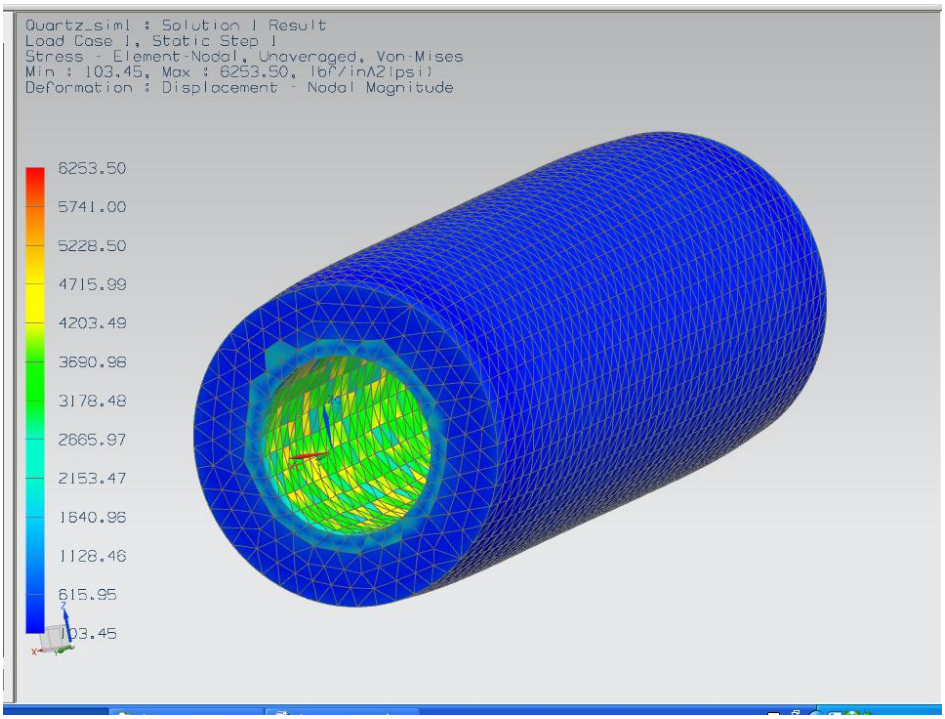

Figure 6 Quartz Tube Stress Analysis

3.3.2 Combustion Chamber

The finite element analysis was then needed to determine the wall thicknesses of the combustor as well as the operational temperature of the combustor walls. The thickness of the combustion wall was found by iterating the wall temperatures and thickness of the stainless steel chamber using NX Nastran Design Simulation until an operating temperature of 350K and a wall thickness of 88.9 millimeters was found to give an acceptable result. A 10 node tetrahedral mesh was used with an overall element size of 12.7 millimeters. This size mesh was checked by performing multiple iterations with decreasing element size and was found to converge on the given results with changes being minimal. The stainless steel properties in the finite element analysis can be found in Table (3) while the FEA results in Fig (7) and Fig (8) show the displacement and stress analysis of the combustion chamber. The fixed constraints placed in the FEA analysis model where located on the outer radial region of the end cap and front cap representative of the constraints placed by the connection to the mounting of the frame limiting the six degrees of freedom. The maximum stress results were 355.08 MPa while the minimum yield strength is 575MPa given for the stainless steel 410. A maximum displacement of 0.13462 millimeters occurs in the mid-section of the stainless steel chamber. Maximum stresses were found inside the window covers corners and edge of the instrumentation ports due to the change of geometry inside the chamber causing stress raisers and creating a region where stress concentration occurs (Budynas et al. 2008)

Table 3 410 Stainless Steel Properties (Azom)

Mechanical Properties

Typical mechanical properties for grade 410 stainless steels are given in table 2.

Table 2. Mechanical properties of 410 grade stainless steel

Tempering Temperature (°C)	Tensile Strength (MPa)	Yield Strength 0.2% Proof (MPa)	Elongation (% in 50mm)	Hardness Brinell (HB)	Impact Charpy V (J)
Annealed *	480 min	275 min	16 min	-	-
204	1310	1000	16	388	30
316	1240	960	14	325	36
427	1405	950	16	401	#
538	985	730	16	321	#
593	870	675	20	255	39
650	755	575	23	225	80

* Annealed properties are specified for Condition A of ASTM A276, for cold finished bar.

Due to associated low impact resistance this steel should not be tempered in the range 425-600°C

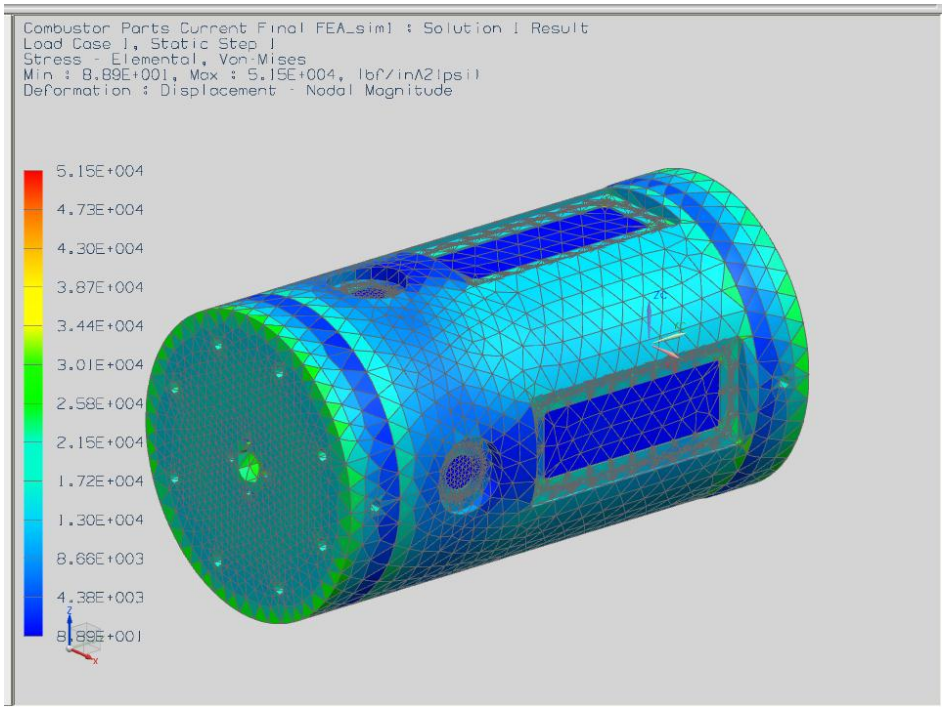

Figure 7 FEA Combustion Chamber

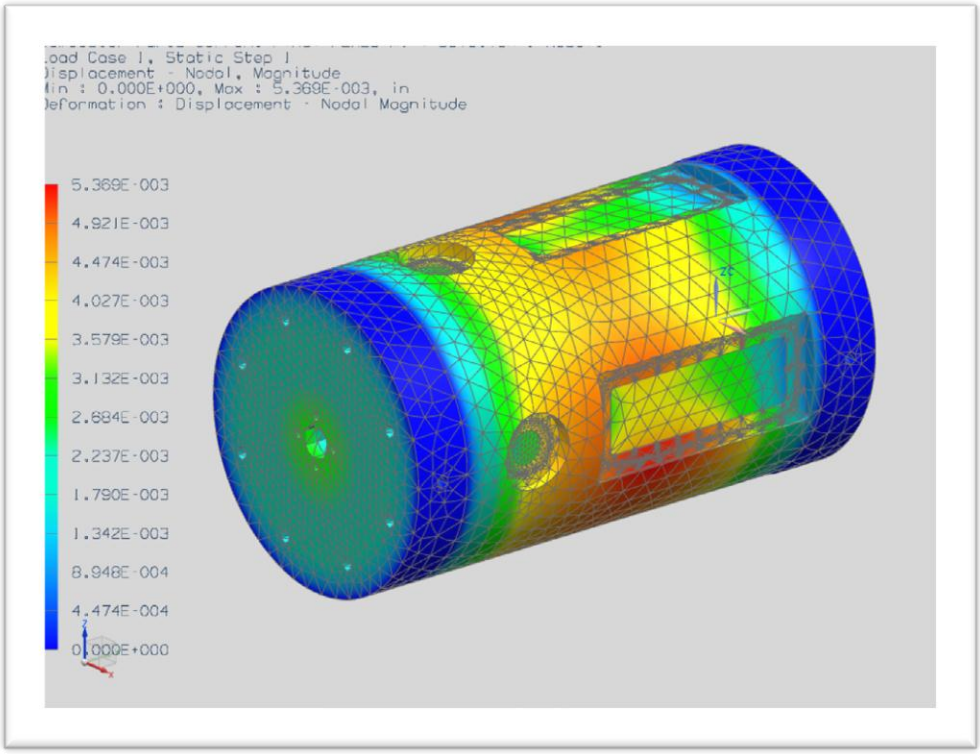

Figure 8 FEA Displacement Combustion Chamber

3.3.3 Window Covers

The finite element analysis of the window covers was conducted. A 10 node tetrahedral mesh was used with an overall element size of 5.08 millimeters. Stainless steel 410 was used and the properties used in the finite element analysis can be found in Table (3) while the FEA results in Figure (8) and Figure (9) show the displacement and stress analysis of the curvature connection. The fixed constraints placed in the FEA analysis model where located on the bolt slots in the window covers representative of the constraints placed by the steel bolts. A temperature load of 350 K and 1.5 MPa pressure was used in the analysis both loads placed on the inner quartz window. The maximum yield strength results where 290.95 MPa while the minimum yield strength of 575 MPa is given for the stainless steel material

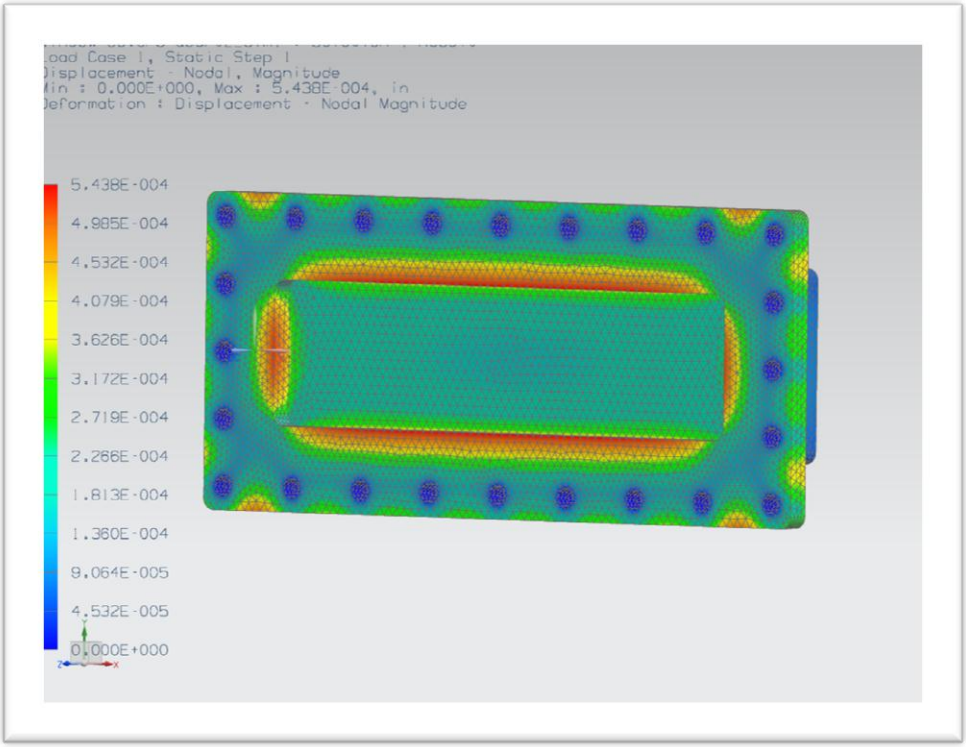

Figure 9 FEA Displacement Analysis Window Covers

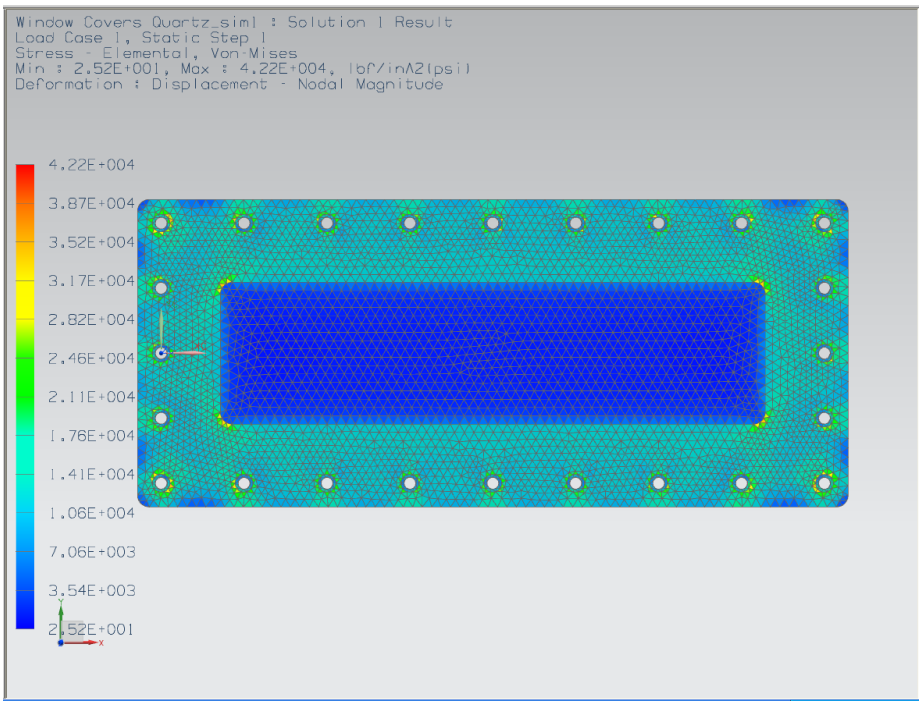

Figure 10 FEA Stress Analysis

3.3.4 FEA of Stand Mounting Connection

The finite element analysis of the design curvature connection between the mounting table and combustor was also needed. A 10 node tetrahedral mesh was used with an overall element size of 5.08 millimeters. The A36 properties in the finite element analysis can be found in Table (4) while the FEA results in Figure (11) and Figure (12) and show the displacement and stress analysis of the curvature connection. The fixed constraints placed in the FEA analysis model were located on the bottom ends of the model representing the constraints placed by the welding of the curvature connection to the table used. A temperature load of 350 K was used and the calculated weight of 76 kN was used to represent the actual weight of the combustor. Also a load of 2.68 kN the maximum calculated force for the thrust created from the combustor, was placed

on the side of the bolt holes representative of the actual operating condition. The maximum stress found was 122.7 MPa while the maximum yield strength of 250 MPa is given for steel A36 material.

Table 4 Steel A36 Properties (Matweb)

Physical Properties	Metric	English	Comments
Density	7.85 g/cc	0.284 lb/in³	Typical of ASTM Steel
Mechanical Properties	**Metric**	**English**	**Comments**
Tensile Strength, Ultimate	400 - 550 MPa	58000 - 79800 psi	
Tensile Strength, Yield	250 MPa	36300 psi	
Elongation at Break	20.0 %	20.0 %	in 200 mm
	23.0 %	23.0 %	In 50 mm.
Modulus of Elasticity	200 GPa	29000 ksi	
Bulk Modulus	140 GPa	20300 ksi	Typical for steel
Poissons Ratio	0.260	0.260	
Shear Modulus	79.3 GPa	11500 ksi	
Component Elements Properties	**Metric**	**English**	**Comments**
Carbon, C	0.25 - 0.290 %	0.25 - 0.290 %	
Copper, Cu	0.20 %	0.20 %	
Iron, Fe	98.0 %	98.0 %	
Manganese, Mn	1.03 %	1.03 %	
Phosphorous, P	<= 0.040 %	<= 0.040 %	
Silicon, Si	0.280 %	0.280 %	
Sulfur, S	<= 0.050 %	<= 0.050 %	

References for this datasheet.

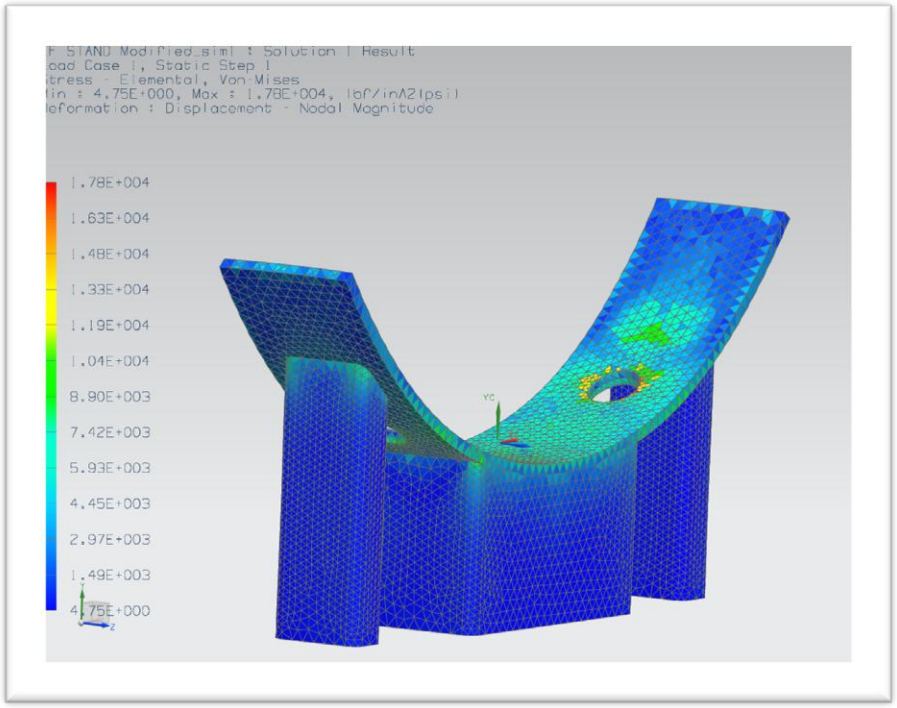

Figure 11 Stress Analysis Curvature Mounting Connection

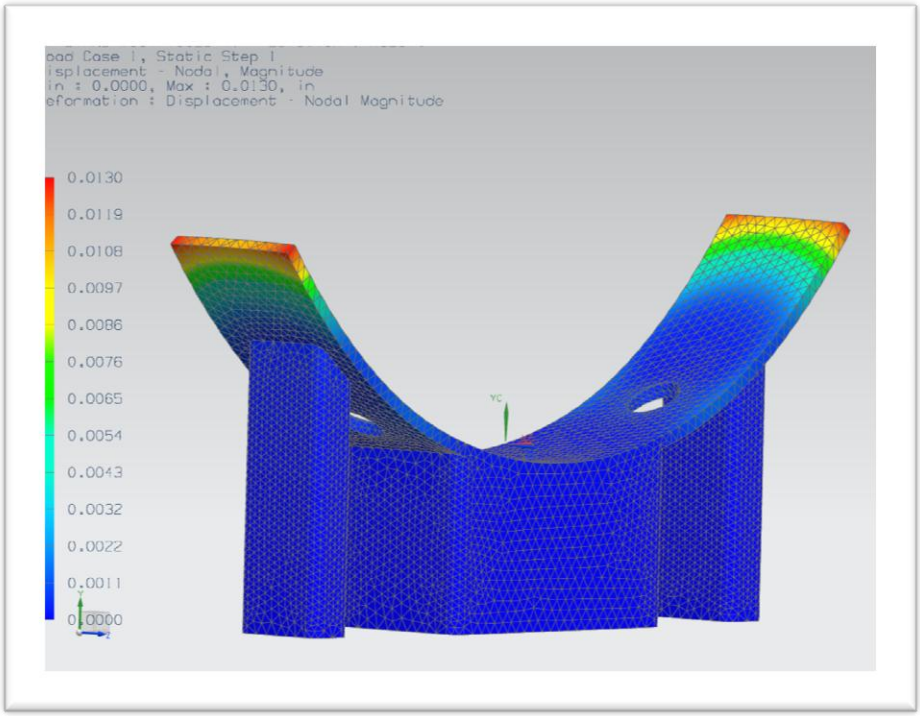

Figure 12 Displacement Analysis Curvature Mounting Connection

3.4 HEAT TRANSFER ANALYSIS

The calculations performed in the previous section show the need to lower the wall temperature of both the combustor wall and the quartz tube. This is accomplished by two cooling methods. One is the use of nitrogen inside the chamber between the outer stainless steel combustor and quartz tube and the other is the use of copper cooling coils filled with running water wrapped around the outside of the combustion chamber.

3.4.1 Quartz Tube Main Combustion Configuration

When operating with the quartz tube inside the stainless steel chamber FEA shows the need to lower the temperature from 2400 Kelvin to 1100 Kelvin in order to avoid failure. This is accomplished with the use of the nitrogen flow inside the combustion chamber. To calculate the heat needed to be removed the use of Equation (3) was used with the specific heat based off of the weight mass fraction sum.

$$q = \dot{m} \int_{T1}^{T2} (X_{CO} C_{p,CO2} + X_{H2O} C_{p,H2O} + X_{N2} C_{p,N2}) dT \quad (3)$$

A total of 162.57 kW was determined to be removed to maintain a safe wall temperature. Equation (4) was then used to calculate the mass flow rate of nitrogen needed to remove 162.57 KW of heat giving us the mass flow rate of .19 kg/s nitrogen needed to bring the temperature of the quartz tube down to 1100K.

$$162.57KW = \dot{m} \int_{300}^{1100} C_{pN_2}\, dT \quad (4)$$

After obtaining the nitrogen flow needed to lower the wall temperature to 1100 Kelvin the next step is to calculate the mass flow rate of water needed to cool down the outer stainless steel chamber. Using Newton's law of cooling seen in Equation (5)

$$\dot{Q}_{conv} = hA_s(T_S - T_\infty) \tag{5}$$

and rearranged to Equation (6)

$$\dot{Q}_{conv} = \frac{(T_S - T_\infty)}{R_{total}} \tag{6}$$

Table 5 Equation 6 Properties

$\boldsymbol{R_{total}}$	$\boldsymbol{.5\ \frac{K}{W}}$
$\boldsymbol{T_S}$	$1100\ K$
$\boldsymbol{T_\infty}$	298 K
$\boldsymbol{R_{conv1}}$	$0.086\frac{K}{W}$
$\boldsymbol{R_{N2}}$	$.33\frac{K}{W}$

Gives a total heat transfer of $\dot{Q}_{conv} = 1604\ W$. Using Equation (7) to solve for the outer surface temperature

$$T_o = T_\infty - \dot{Q_{conv}}\ (R_{conv1} + R_{N2}) \tag{7}$$

we obtain an outer surface temperature of $T_o = 364$ K. Using Equation (3) a total of 1.28 kW of heat are needed to be removed. Then using Equation (8)

$$1.28\ KW = \dot{m} \int_{300}^{350} C_{pH20} dT \quad (8)$$

We obtain a total mass flow rate of .008 kg/s of H_2O needed to lower the outer stainless steel wall temperature form 364K to 350 K. The low mass flow rate of water needed outside the chamber is due to the inner cooling use of nitrogen inside the chamber.

3.4.2 Stainless Steel Main Combustion Chamber Configuration

When operating with the stainless steel chamber as the main combustion chamber the wall temperatures can theoretically be 2400 K was determined. Due to these high temperatures the need to cool the combustion walls to 350 K was determined finite element analysis. Using Equation (3) the total amount of heat needed to be removed was found to be 393 KW. The mass flow rate of H_2O needed to remove the heat is then calculated using Equation (9) this corresponded to a water flow rate of 1.21 kg/s and the calculations can be seen in Appendix E. Also included is the use CFD model using FLUENT simulating the use of a 2.54 cm thickness cooling jacket showing the relationship of the mass flow rate and temperature under a constant heat flux load and can be found in Appendix F.

$$388.31KW = \dot{m} \int_{273}^{350} C_p\, dT \quad (9)$$

3.5 PUMP SIZING AND MASS FLOW ANALYSIS

Once the maximum mass flow rate was calculated the next step was to calculate the head losses occurring in the piping system and the sizing of the pump was needed. The proposed cooling system will incorporate the use of a 2,200 liter holding tank for the water, a 3.81 cm diameter pipe acting as the connection from the tank to the pump and from the main combustion chamber

to the discharge line, as well as .635 cm diameter pipe that will wrap around the combustor as shown in Figure (13). If operating for 30 minutes a total of 2,167 liters would be used.

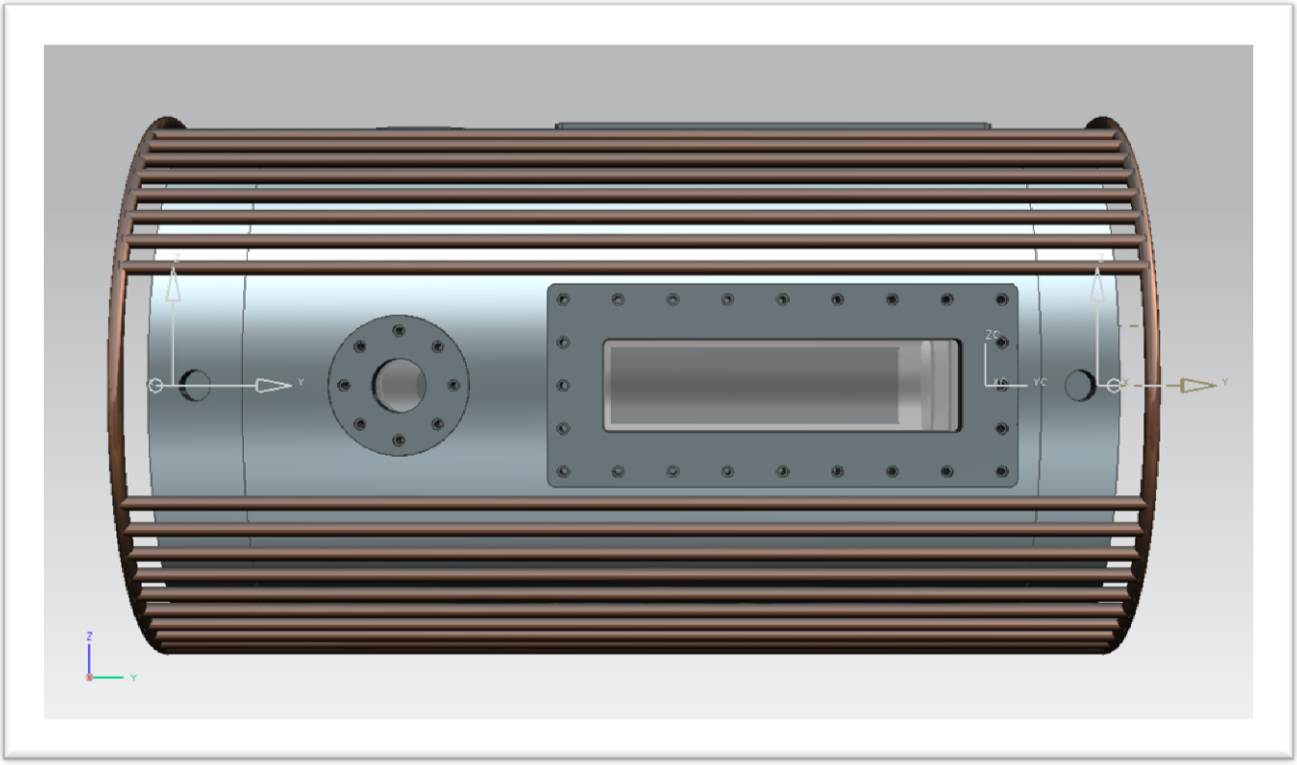

Figure 13 Cooling Coil

Bernoulli's equation shown in Equation (10) was used to calculate the head losses.

$$\frac{P_1}{\gamma} + z_1 + \frac{v_1^2}{2g} + h_A - h_L = \frac{P_2}{\gamma} + z_2 + \frac{v_2^2}{2g} \tag{10}$$

Where h_L includes the losses that occur due to entrance loss, friction loss in the 3.81 cm diameter and .635 cm diameter line, valve fitting, 90 degree angle elbows, flow through branch losses, and the exit loss occurring. An assumption of 10 meter of 3.81 cm steel pipe was assumed and 20 meters of .635 cm diameter pipe was assumed to be used in the cooling wrap of the combustor. A total of four 90 degree angle elbows at 3.81 cm diameter where assumed, and 80 flow through branches where assumed to be used in the wrap around the combustor. Also an elevation

difference of 1.2 meters where assumed to occur between the exit discharge line to the top of the storage tank limit. A total of 9.37 meters of head loss was calculated to occur using the assumed conditions. The pump sizing was calculated using Equation (11) and was found to be 145 W pump needed assuming .76 pump efficiency. Complete calculations and values can be found in Appendix E. When operating at 1.21 kg/s and under the assumption stated the use of a cast iron centrifugal pump from Macmasters part number 99435k23 would be recommended with the power output being 550 W and a mass flow of 132 Liters/minute while operating at 18.28 meters of head.

$$Power = \frac{h_A \gamma Q}{E_f} \tag{11}$$

4. Experimental Results

The results of the project will bring a unique testing facility that will allow future research in flame characteristics of coal derived fuels of turbine combustors.

Some initial factors considered included cost analysis, operating temperatures, operating pressure, dimensional restraints, weight restraints, safety assurance, and feasibility of manufacturability of the final project. The main design parameters considered for this application included a chamber operating pressure of 1.5 MPa and temperature of 2400 K. These must be maintained while designing for safety assurance, dimensional restraint, weight, safety assurance, and feasibility. This temperature and pressure were selected due to the high hydrogen fuel composition that will be used in testing as well as the pressure representative of an actual gas turbine.

The parameters define the synthesis stage of the design. Various preceding design concepts were researched and investigated as well as independent proposals for the design was undertaken. Each concept was analyzed, revised, improved, or discarded as the project progressed in an effort to optimize the best design where all the set parameters are met.

Evaluation of the design is completed through a pressure leakage test. The design phases taken from Budynas et al (2008) are summarized in Figure (14) and show the different feedbacks and iterations of each stage.

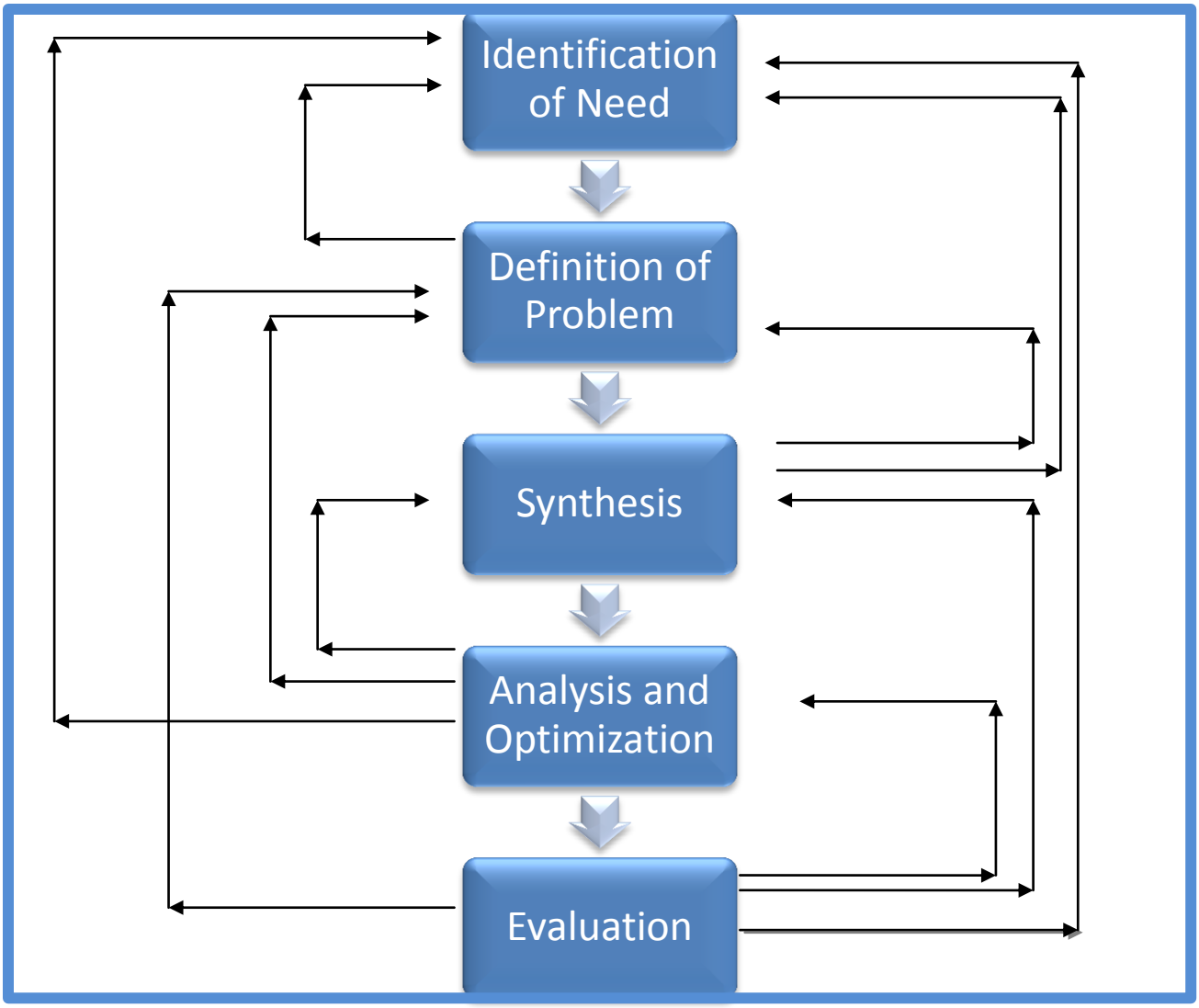

Figure 14 Design Process (Budynas 2008)

The description, dimensions, and purpose of each combustor part will be covered in the upcoming sections. The overall design of the combustor can be seen in Figure (15) and Figure (16) and include the three main sections of the combustion chamber. The end cap, main combustion chamber, front cap, as well as various other components that were implemented in the design.

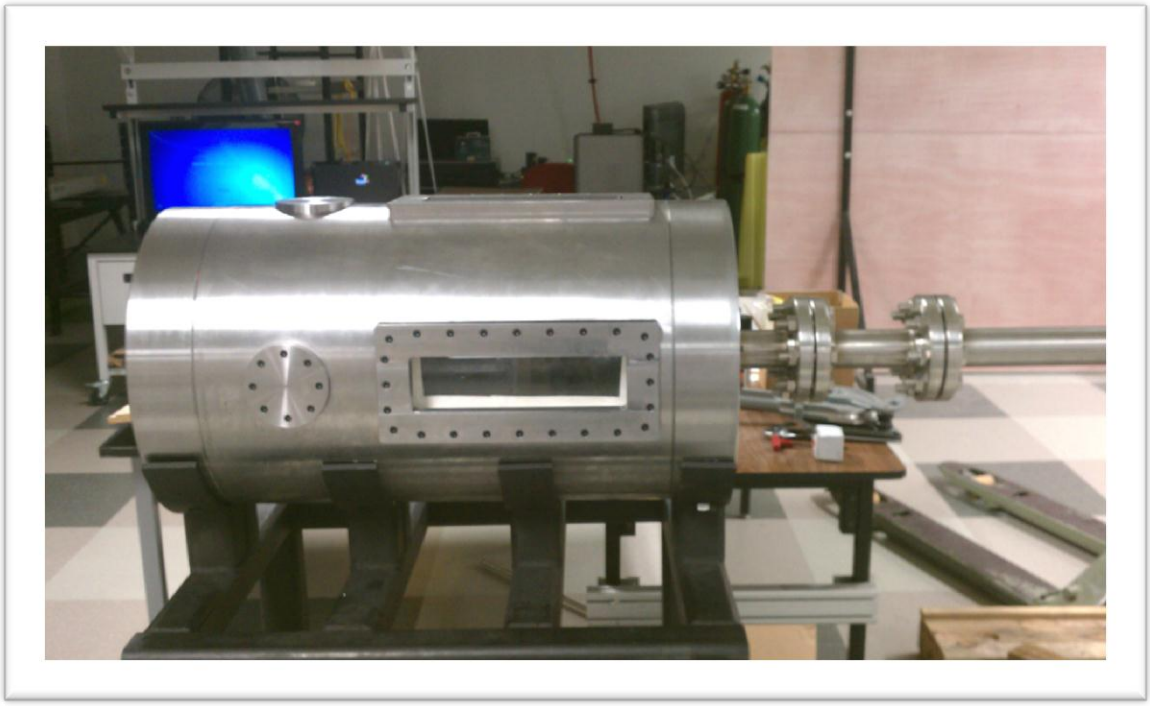

Figure 15 Overall Design of Combustion Chamber

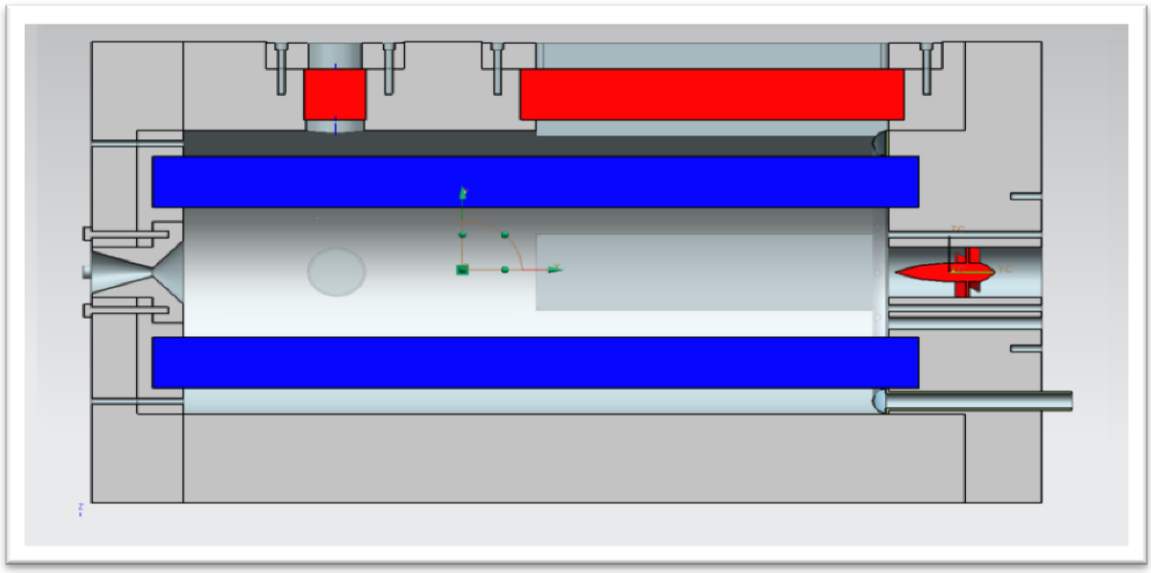

Figure 16 Inside Schematic of Combustion Chamber

4.1 INLET MANIFOLD

The combustion process in some types of gas turbine can be classified into two types of combustion. The first being a diffusion flame where the fuel air mixture occur in the combustion chamber. The other is lean-premixed combustion where the fuel and air are previously mixed away from the combustor section in an effort to obtain lean, uniform, unburned fuel/air mixture [EPA 2000].

The combustor developed will be using a lean-premixed combustion process. The fuel and air is mixed in the inlet manifold and then sent to the main combustion area. The inlet manifolds main purpose is to act as a mixing area for the fuel and air mixture and to reduce injection induced flow irregularities.

4.1.1 Design Description and Dimensions

The inlet manifold in Figure (17) is compromised of three modular sections. The first acting as the fuel/air inlet mixture section. The second is a removable static mixture section which is composed of horizontal tubes located inside the chamber that remove irregularities and provide an improvement towards laminar flow. This section is then attached to third section which connects the inlet manifold to the main combustor section. The use of flanges are used as connections between the inlet manifold, three modular sections, and the use of 6.35 millimeters bolts connect the inlet manifold to the combustor connecting front cap. There is also a pressure blow out valve located at the third modular section to provide a level of safety in case of malfunction and an increase of pressure.

The given dimension of the inlet manifold is a 54.5 cm in total length with the three modular section composed of 35 cm length for the inlet/initial mixture zone, 11.5 cm in length for the

static mixture section, and 7.6 cm length for the connecting section. The inner diameter of the piping is 5.08 cm with a 6.35 mm thickness for all three sections. The material chosen was stainless steel 316 due to availability and an FEA stress analysis resulting in adequate results.

Figure 17 Inlet Manifold

4.1.2 Combustor Operation

The fuel enters through four alternative injection holes located in the inlet section of the manifold and is supplied by fuel and tanks. The compressed air enters trough one inlet located next to the fuel injection ports supplied by a high pressure compressor. The fuel and air then enter into the inlet manifold where initial mixing occurs then pass through a static mixture section that assists in eliminating injection induce flow irregularities while insuring laminar flow. From this section the flow is then directed to the main combustor.

4.2 FRONT CAP

The front cap of the combustor can be seen in Figure (18) and Figure (19) and acts as an inlet to the main combustor chamber. It houses the ignition system, the swirler, instrumentation holes, and connects the inlet manifold to the main chamber.

4.2.1Design Description and Dimensions

The front cap is composed of one solid section and the draft with the exact dimensions can be seen in Index C. The outer radius is 0.4572 meters with a 0.0508 m to 0.0381 m ratio converging nozzle in the mid section of the model. The use of a converging nozzle is used to house the swirler and allow the passage of fuel and air mixture into the main combustion chamber. The use of eight 12.7 millimeters diameter bolts are used to connect the end cap to the main chamber while the use of 6.35 millimeters diameter bolts are used to connect the inlet manifold to the front cap. The combustor will operate under two different configurations. One includes the use of a quartz tube and will be held in place in part by the front cap while the circular pocket seen in Figure (17) is intended to hold the quartz tube in place.

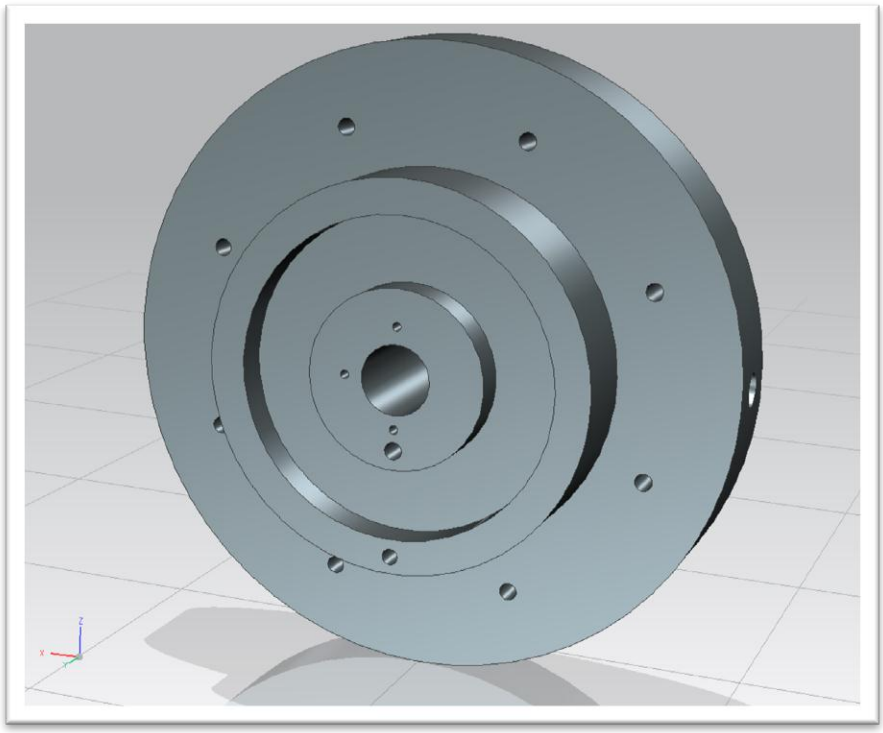

Figure 18 Front Cap With Quartz Configuration Slot

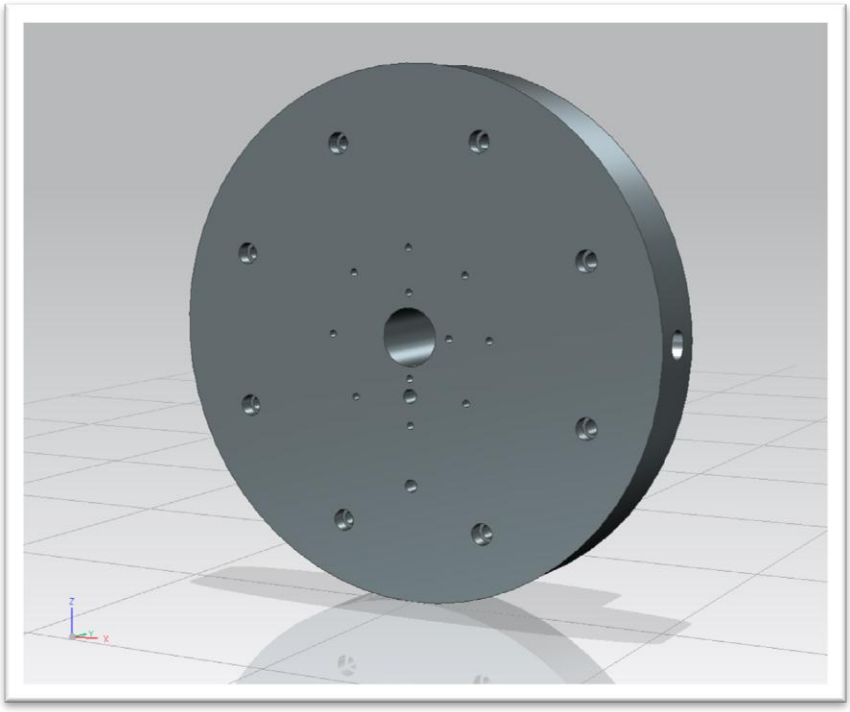

Figure 19 Front Cap Connecting Side to Inlet Manifold

4.2.2 Ignition System

The ignition system is located in the main combustion chamber and the CAD model can be seen in Figure (20). The use of a spark plug and methane will be used in the igniter and is currently still being developed for the system. A 19.05 millimeters diameter hole that runs through the end cap will hold the igniter in place and will provide the flame needed for ignition right below the main fuel and air entry point.

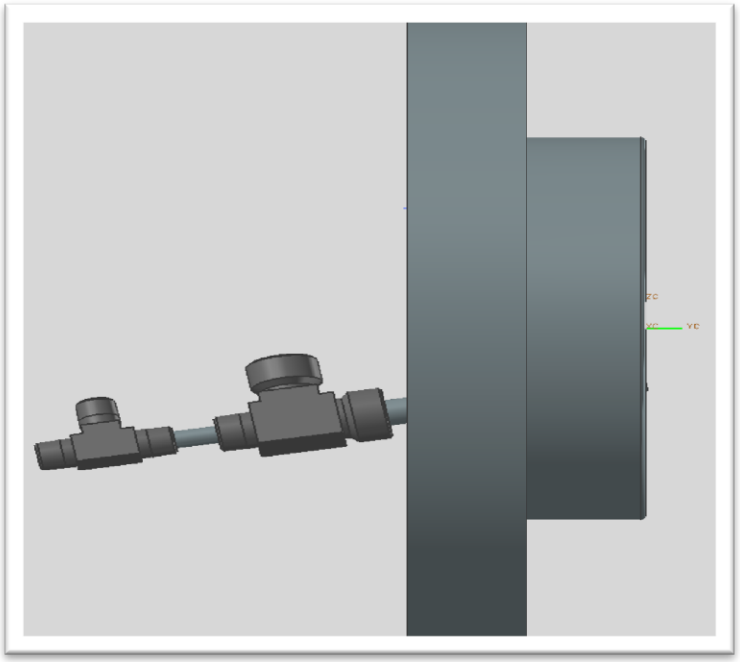

Figure 20 Ignition System

4.3 AIR DISTRIBUTOR

One of the operational configurations of the combustor employs a quartz tube inside the stainless chamber as the main combustion compartment. Due to high thermal stress, subjected to the quartz chamber, it is then necessary to cool the outer quartz chamber with the use of nitrogen. The need for a nitrogen distributor was then developed to provide even distribution of nitrogen along the outer quartz chamber.

4.3.1 Design Description and Dimension

The distributor is hollow in the inner section to allow the flow of air and also has a connecting tube attached to it where the flow intake of air will originate. There are a total of sixteen distribution holes with eight of them being pointed an 90 angle and the other eight pointed towards 180 degree angle towards the quartz outer chamber wall. The design layout can be seen in Figure (21) while the cooling system flow diagram for the quartz tube can be seen in Figure (22)

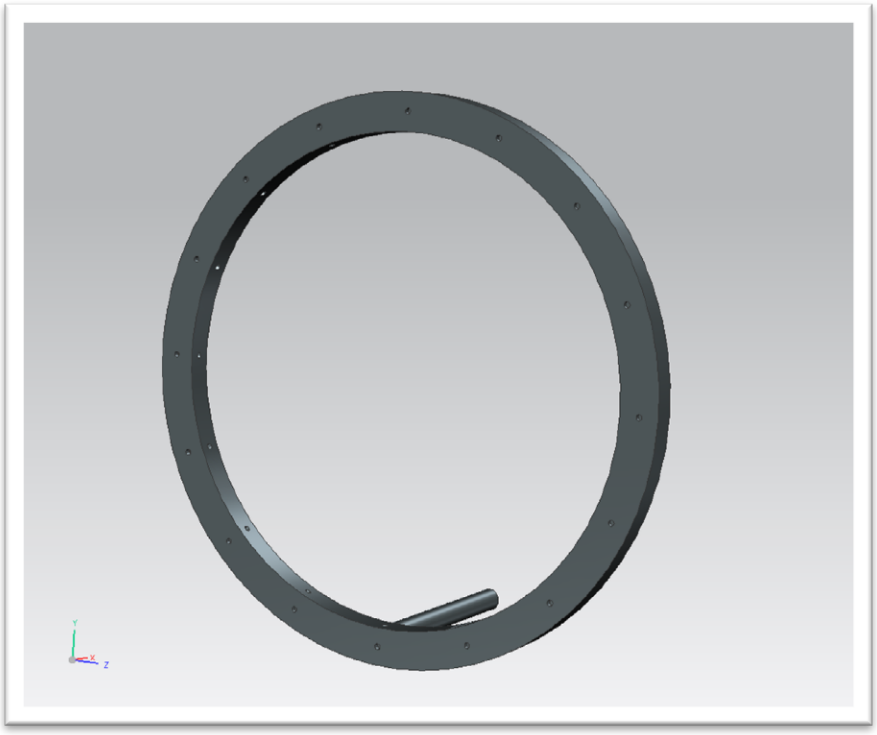

Figure 21 Nitrogen Distributor

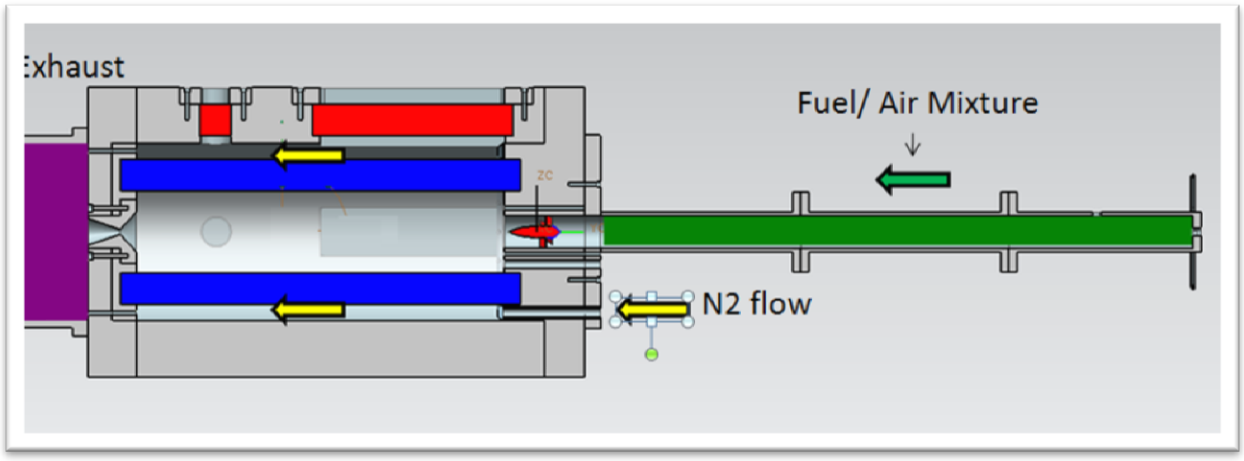

Figure 22 Nitrogen Fuel/Air Flow Schematic

4.4 STAINLESS STEEL COMBUSTION CHAMBER

The main combustion chamber houses the combustion of the fuel and is required to withstand the high temperatures as well as the operational pressure that will be needed to conduct the various experiments. The chamber also houses the windows that are needed to give optical access to the combustion as well as various instrumentation ports to take needed data used for experimentation.

4.4.1 Design Description and Dimension

The combustor has an inner diameter of 0.2794 meters with an 88.9 millimeters thickness. The total length of the combustor is 0.6477 meters. Three window ports are located on the two sides and top of the combustor evenly spaced by 90 degrees off center. The rectangular window slot dimensions are composed of 317.5 millimeters by 101.6 millimeters length and width with an additional tolerance of .5 millimeters given to each side to allow the placement of a gasket. Three circular ports with 50.8 millimeters diameter will allow for either instrumentation devices to be located or for a circular viewing port at the outer end of the combustor. Eight 1.27 cm diameter threaded holes are located at each end of the combustor to allow the connection of the

front cap and end cap that will make up the combustor as a whole. The main material used is stainless steel 410 due to the high yield stress and desired characteristics compared to other stainless steel material. The side, angled, and front view of the combustor can be seen in Figure (23), Figure (24), and Figure (25) respectively.

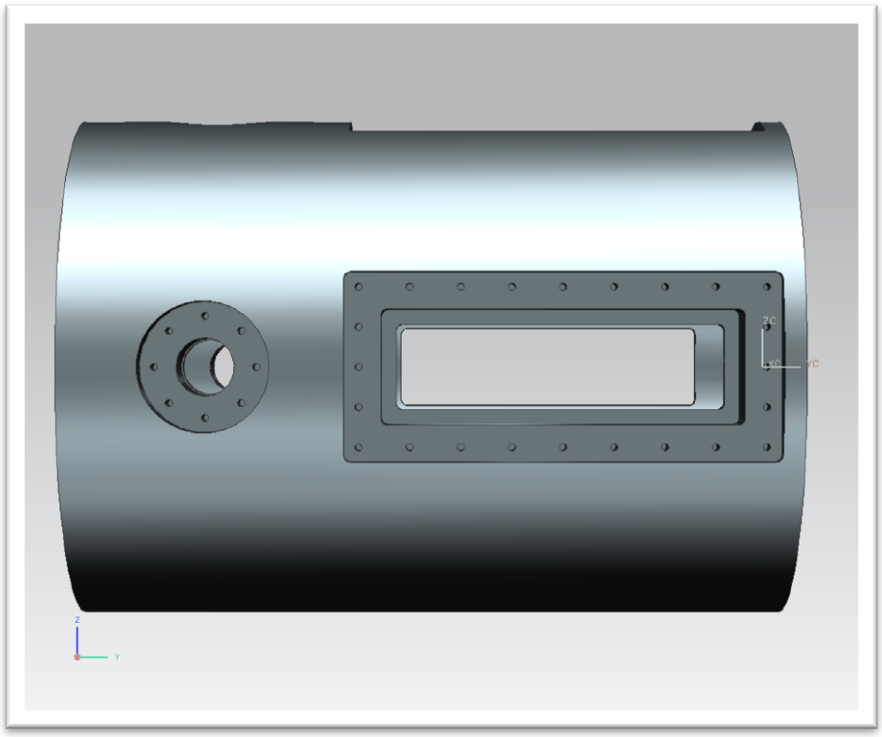

Figure 23 Combustor Stainless Steel Side View

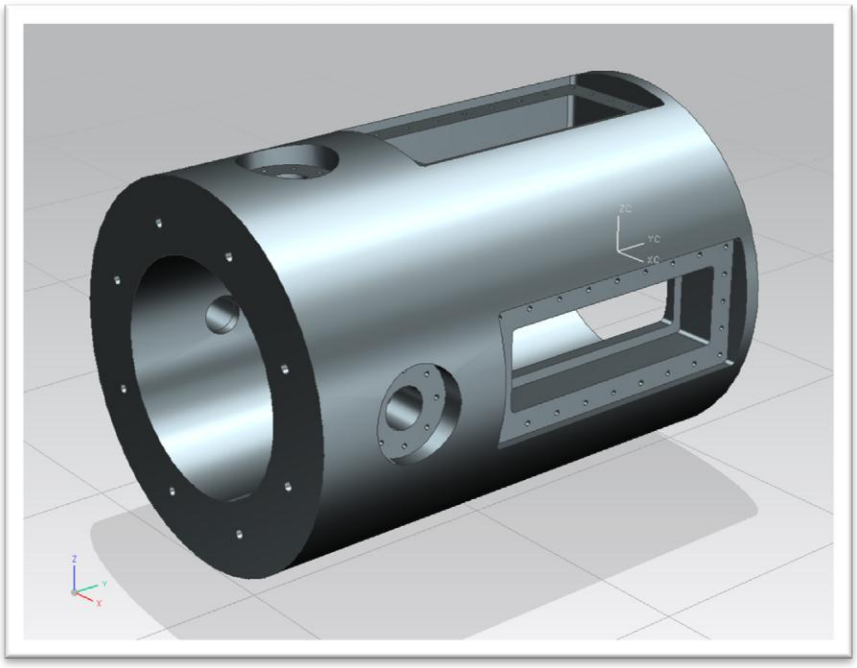

Figure 24 Stainless Steel Chamber

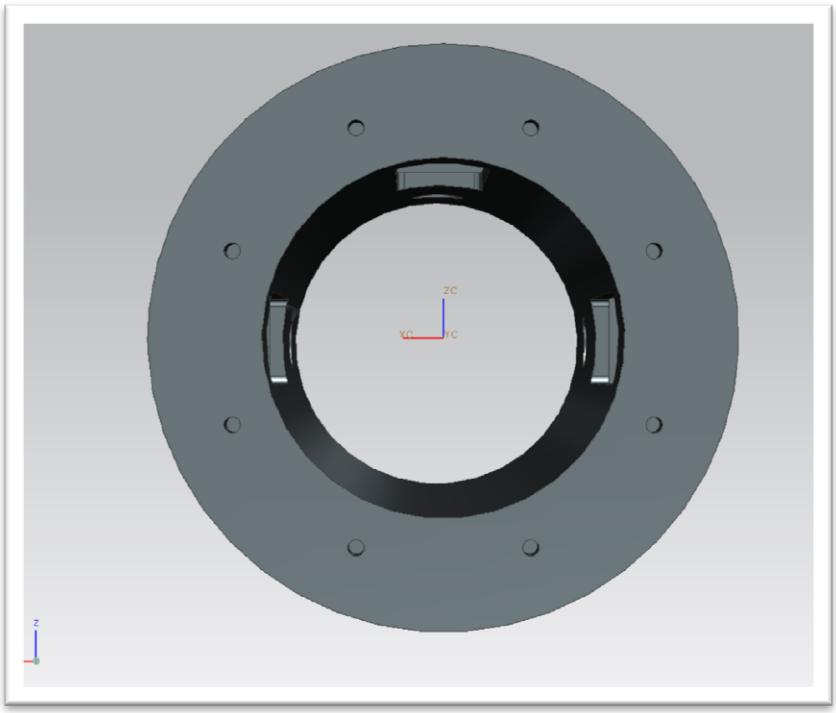

Figure 25 Stainless Steel Chamber Front View

4.5 WINDOW COVERS/ INTERCHANGEABLE INSTRUMENTATION PORTS

4.5. 1Purpose and Design Dimensions

The window covers are needed to hold down the rectangular quartz windows. The outer dimensions of the covers are made up of 16.51 cm by 38.1 cm length and width while the inner dimensions are composed of 10.16 cm by 29.21 cm with an overall 2.54 cm thickness. The windows covers will be attached to the combustor by the use of 24 6.35 millimeters diameter bolts. The design configuration can be seen in Figure (26)

The instrumentation ports will be used for both optical accesses as well an interchangeable port for the placement of thermocouple, burst disk, and or pressure transducer. It will also allow for easy access to the inner combustion chamber and can be used as an entry point to do material testing inside the combustor. The use of eight 12.7 millimeters diameter bolts are used to secure ports in place. Figure (27) showing the circular port cover used when operating as a window, and Figure (28) and Figure (29) showing the cover used when operating as an instrumentation port. Both window cover and instrumentation ports are made of 410 stainless steel conforming to the combustor and inlet and end cap material.

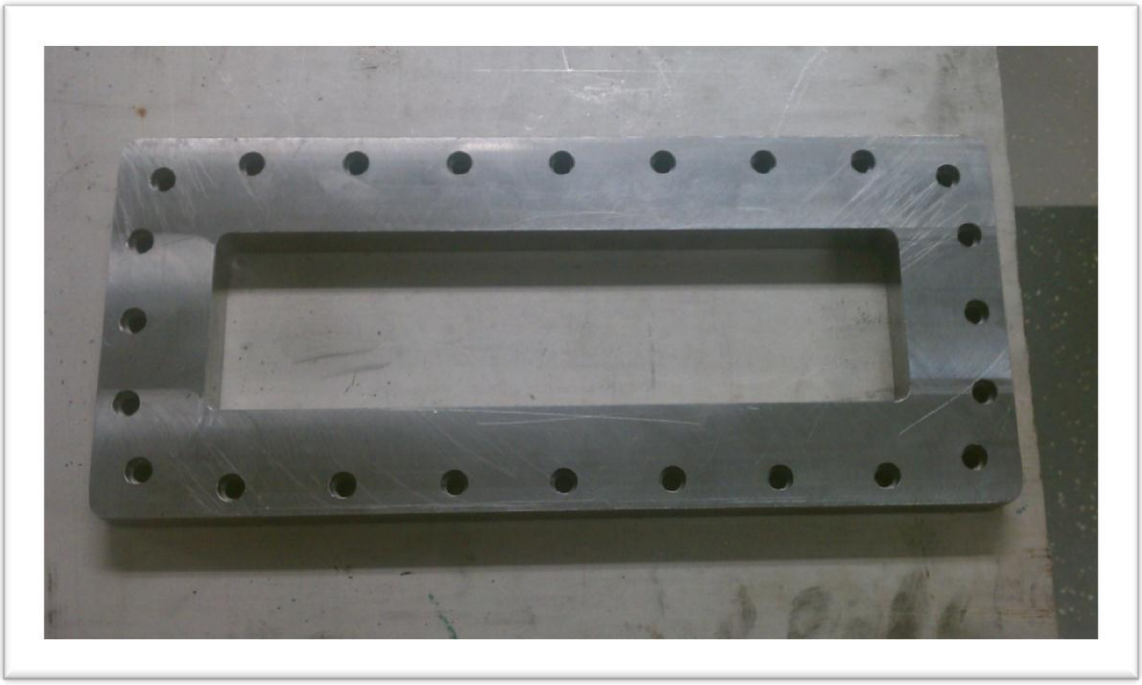

Figure 26 Stainless Steel Rectangular Window Cover

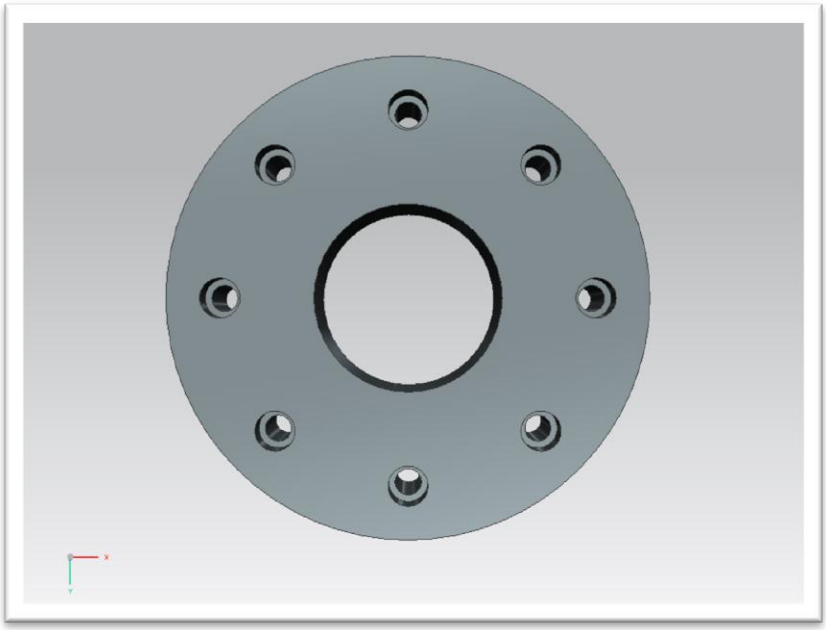

Figure 27 Stainless Steel Round Window Cover

Figure 28 Stainless Steel Instrumentation Port

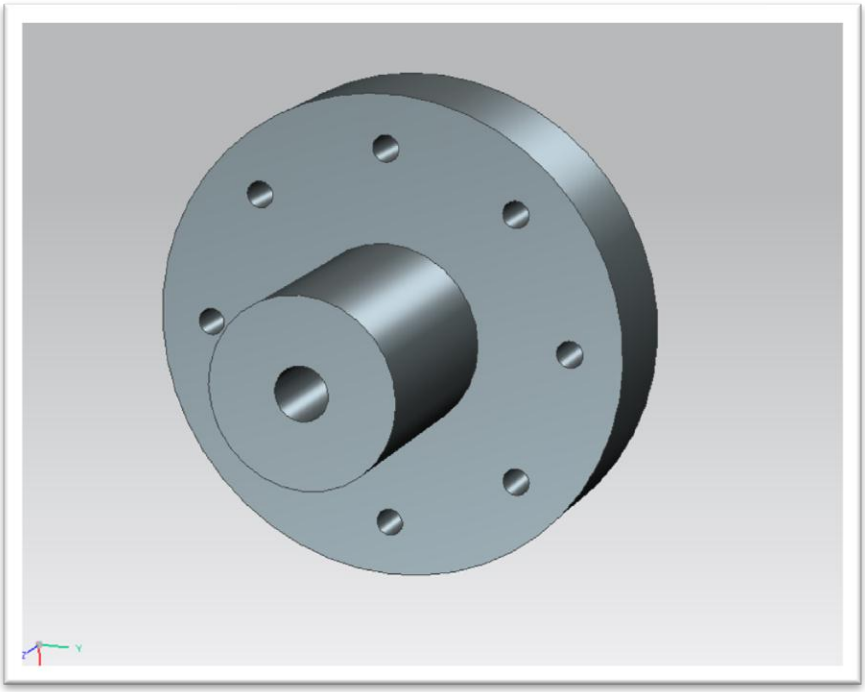

Figure 29 Stainless Steel Instrumentation Port Inner View

4.6 CYLINDRICAL QUARTZ TUBE AND RECTANGULAR WINDOWS

4.6.1 Purpose and Design Dimensions

The combustor is designed to operate under two distinct conditions. One is with the use of a quartz tube acting as the main combustion chamber. The other is with the tube removed allowing the stainless steel chamber to act as the main chamber. This allows for different configurations to show how the burner geometry can affect flashback as well as NOx emission due to being dependent on burner design.

The quartz tube used has an outer diameter of 22.86 cm, inner diameter of 12.7 cm and a total length of 63.5 cm. The use of three rectangular quartz windows is also incorporated with the outer stainless steel chamber for visual based instrumentation. The quartz rectangular quartz windows are 31.75 cm in length with 5.08 cm thickness and 10.16 cm width with a 6.35 millimeters circular grove on the four corners.

The quartz windows were purchased from Machined Glass Specialist Inc. and were manufactured from Heraeus Quarzgla Solutions and are TC3© fused quartz. The technical properties can be found in Appendix B with the transmission spectrum shown in Figure (30). The wavelength for particle image velocimetry (PIV) used are at 532 nm giving a transmission percentage of approximately 90% allowing the use of the TSC3 quartz glass manufactured.

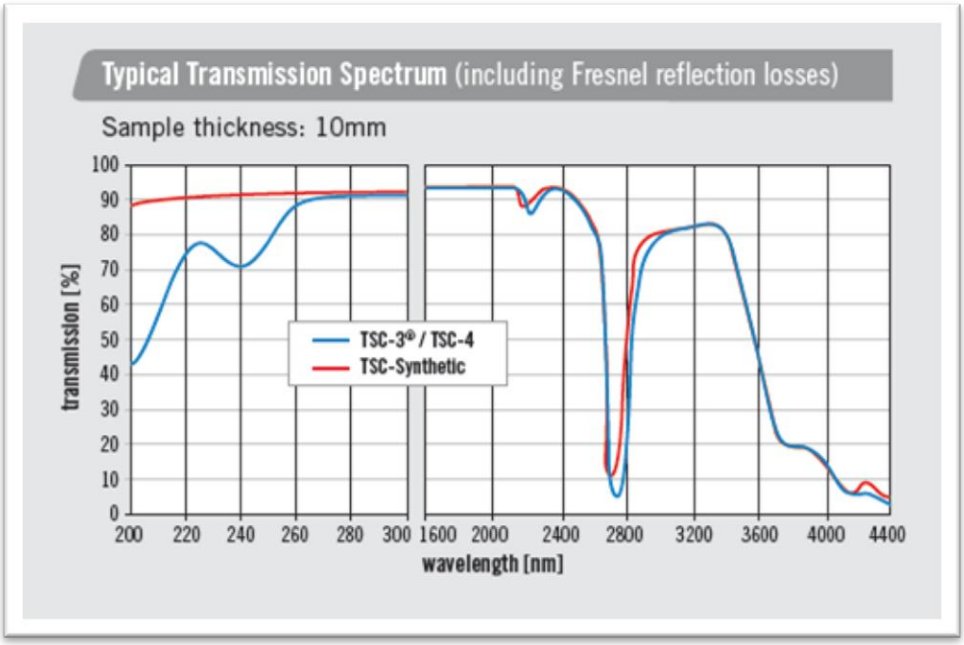

Figure 30 Quartz Transmission Spectrum

Figure 31 Square Quartz Windows

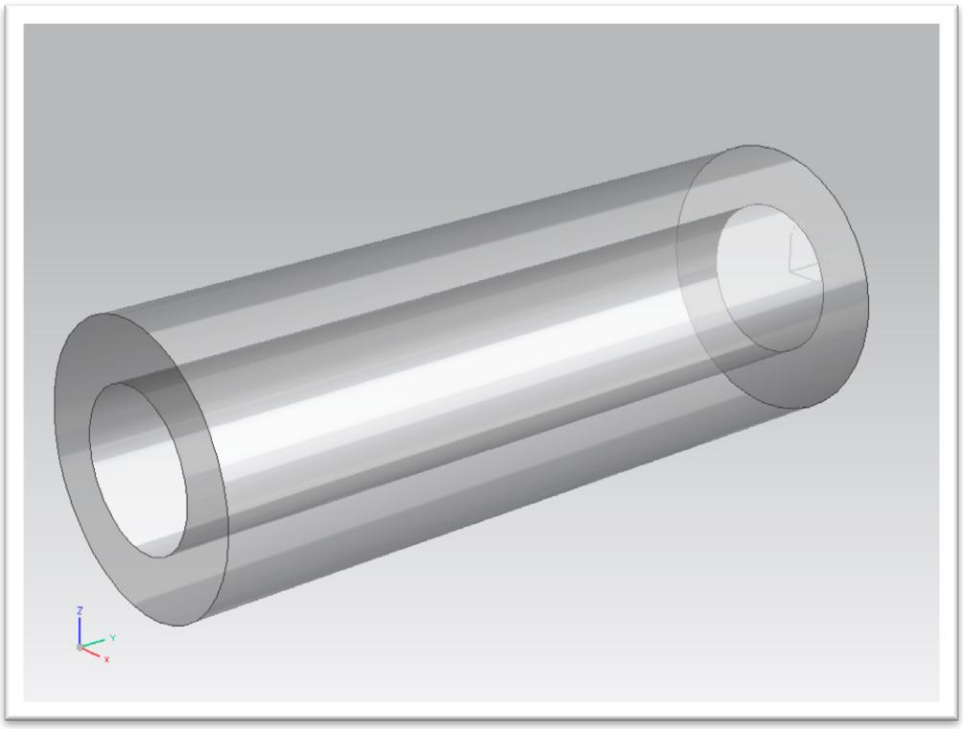

Figure 32 Inner Quartz Tube

4.7 END CAP

The end cap is made of up of three removable modular sections. They include the converging nozzle, the nitrogen exhaust disk, and the outer main cap that connects the end cap to the main combustion chamber. The three part assembly is shown in Figure (33). Although the current status the end cap is designed in a way that the listed design below can be manufactured to fit the existing parts.

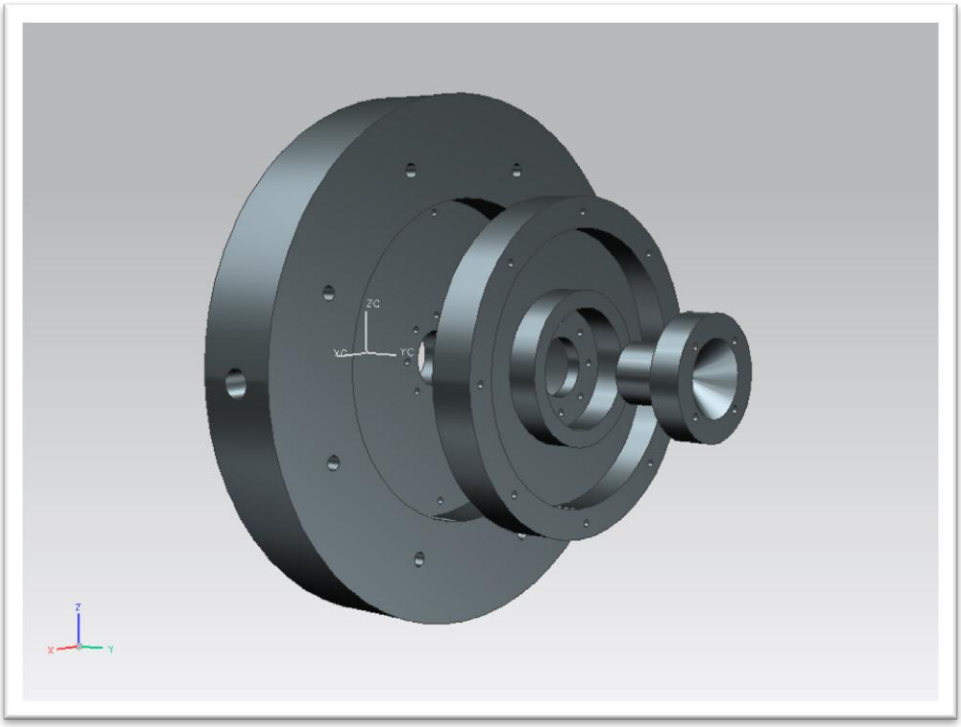

Figure 33 End Cap Assembly

4.7.1 Converging Nozzle

The main purpose of the converging nozzle is to control the pressure drop across the combustor. The throat area was calculated using Equation (12) and was found to be 161.29 mm^2. The design can be seen in Figure (34) and Figure (35) back and front view while being attached to the main combustion chamber using interlocking parts and 4 6.35 millimeters diameter stainless steel bolts.

$$A_T = \frac{\dot{m}\sqrt{RT_T}}{P_T\sqrt{\gamma}\,Ma}\left(1 + \left(\frac{\gamma-1}{2}\right)Ma^2\right)^{\frac{\gamma+1}{2-2}\gamma} \quad (12)$$

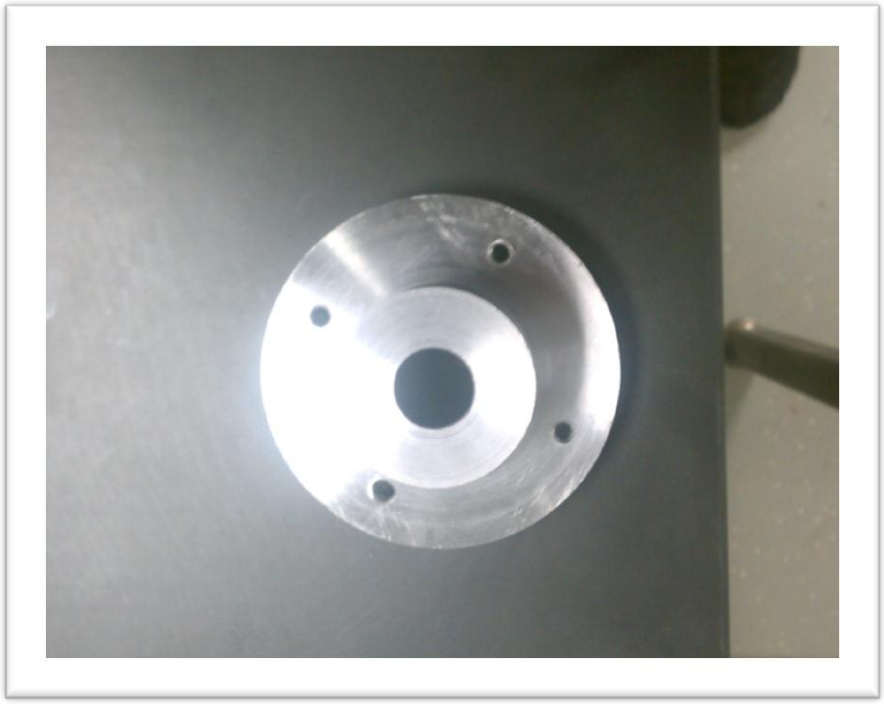

Figure 34 Exit Nozzel Bolt View

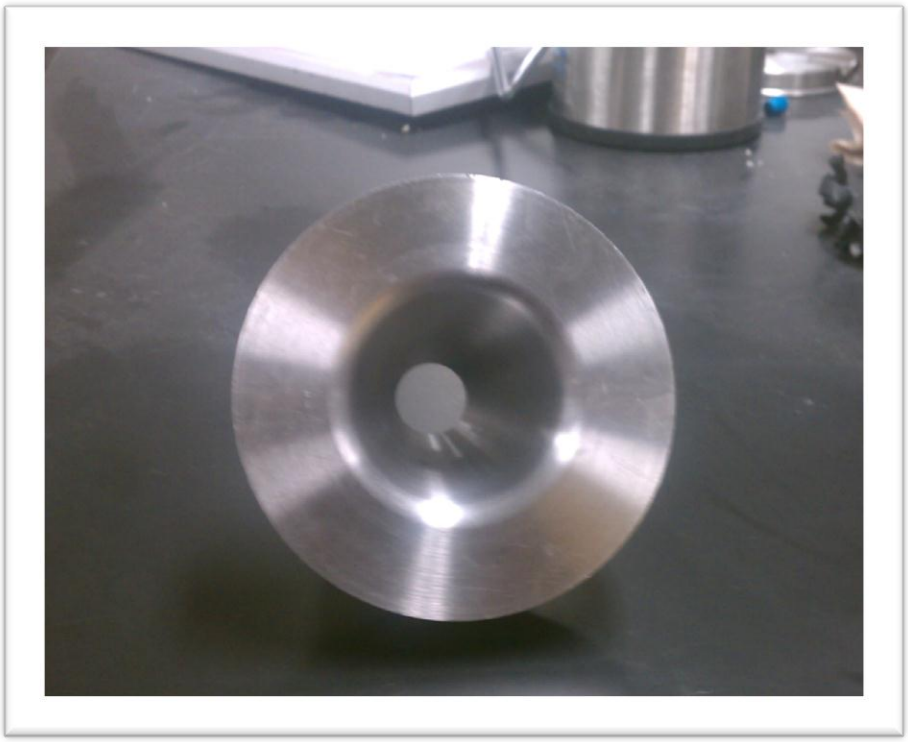

Figure 35 Exit Nozzle

4.7.2 Nitrogen Exhaust Disk

The nitrogen exhaust disk is needed when operating with the inner quartz tube configuration. This disk will align with the end cap exhaust ports and allow nitrogen flow to exit through the end cap. When the quartz tube is not in use and the nitrogen flow is not needed then it will possible to replace the nitrogen exhaust disk to a solid circular piece that will block the fixed nitrogen ports on the end cap. Both arrangements can be seen in Figure (36) and Figure (37).

The disk will be connected to the main end cap and CD nozzle through 6.35 millimeters diameter stainless steel bolts that will run along the modular sections. The pressure created in the combustor chamber and the use of grouping will also help in the sealing of the nitrogen exhaust disk.

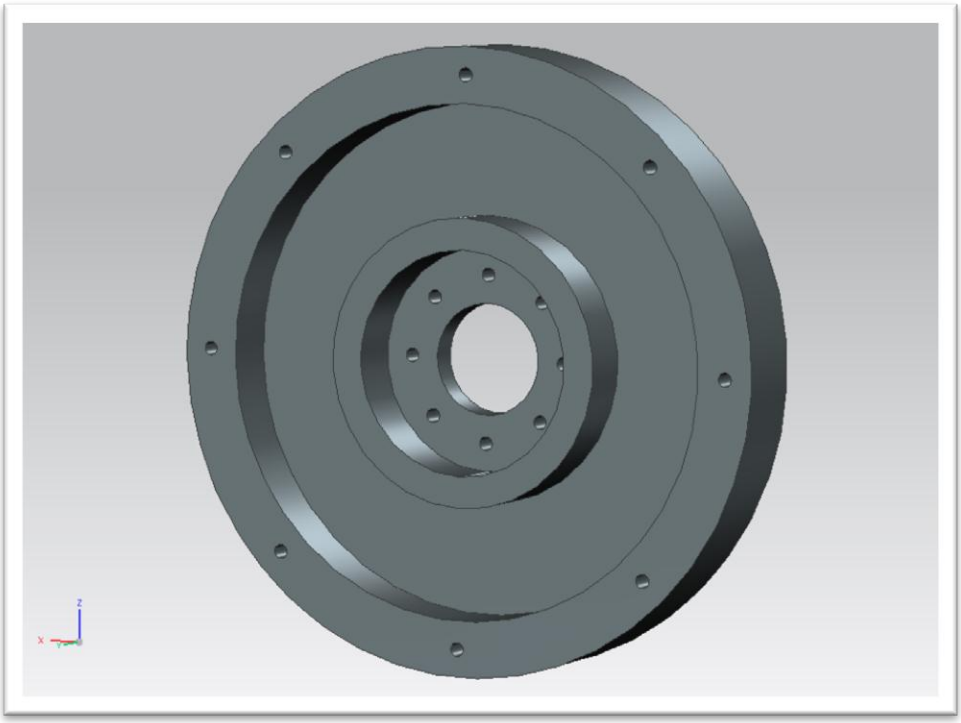

Figure 36 Nitrogen Exhaust Disk

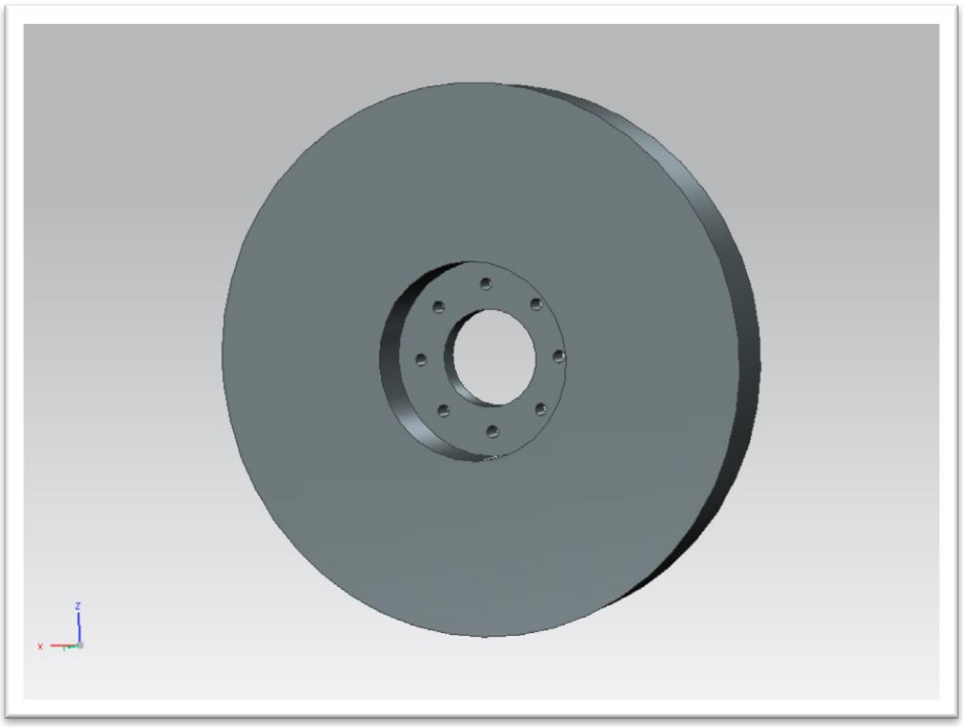

Figure 37 Solid Disk When Operating Without Nitrogen Cooling Flow

4.7.2 Main End Cap

The main end cap acts as a sealant to the main combustion chamber. It is also the link between the combustion chamber and the exhaust. The outer dimension is 0.4572 meters with a hole with a 50.8 millimeters diameter for the converging nozzle exhaust port. Also 16 ports for the nitrogen exhaust ports of the cooling system of the inner combustor are also located on the end cap. The end cap will be attached to the main combustor by 8 12.7 millimeters diameter stainless steel bolts. The design set up is seen in Figure (38).

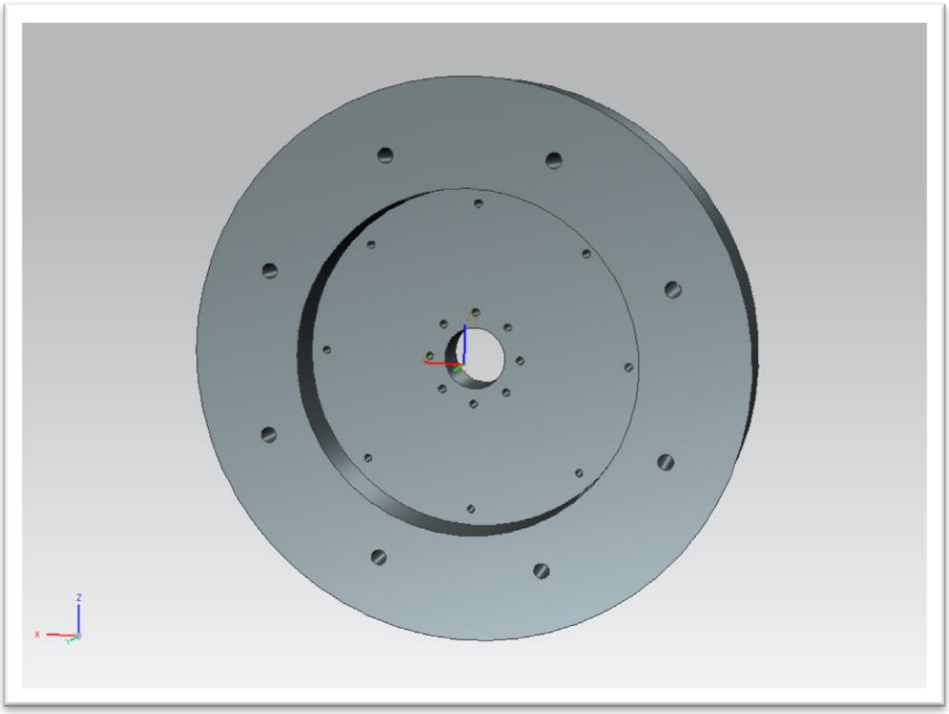

Figure 38 Main End Cap

4.8 BOLT SPECIFICATION

The bolts used are medium carbon grade 8 alloy steel conforming to ASTM A574 with a minimum Rockwell hardness of C39, minimum tensile strength of 1241.05 MPa, a proof strength of 965.26 MPa, and minimum yield strength 1054.89 MPa. All bolts have a black oxide finish that gives the bolt rust resistance.

The use of eight 12.7 millimeters diameter bolts are used on each the end cap and front cap providing the connection to the main combustion chamber. A total of twenty-four 6.35 millimeters diameter bolts are used to secure each window cover with a total of seventy-two bolts used. The instrumentation ports use eight 6.35 millimeters diameter bolts each with a total of twenty-four bolts used. In addition eight 6.35 millimeters diameter bolts are used to connect

the exhaust and inlet manifold to the end cap and inlet cap respectively. The bolts were purchased from MacMasters and CAD drawing with dimensions can be seen in Figure (39) for the 12.7 millimeters diameter bolts and Figure (40) for the 6.35 millimeters diameter bolts.

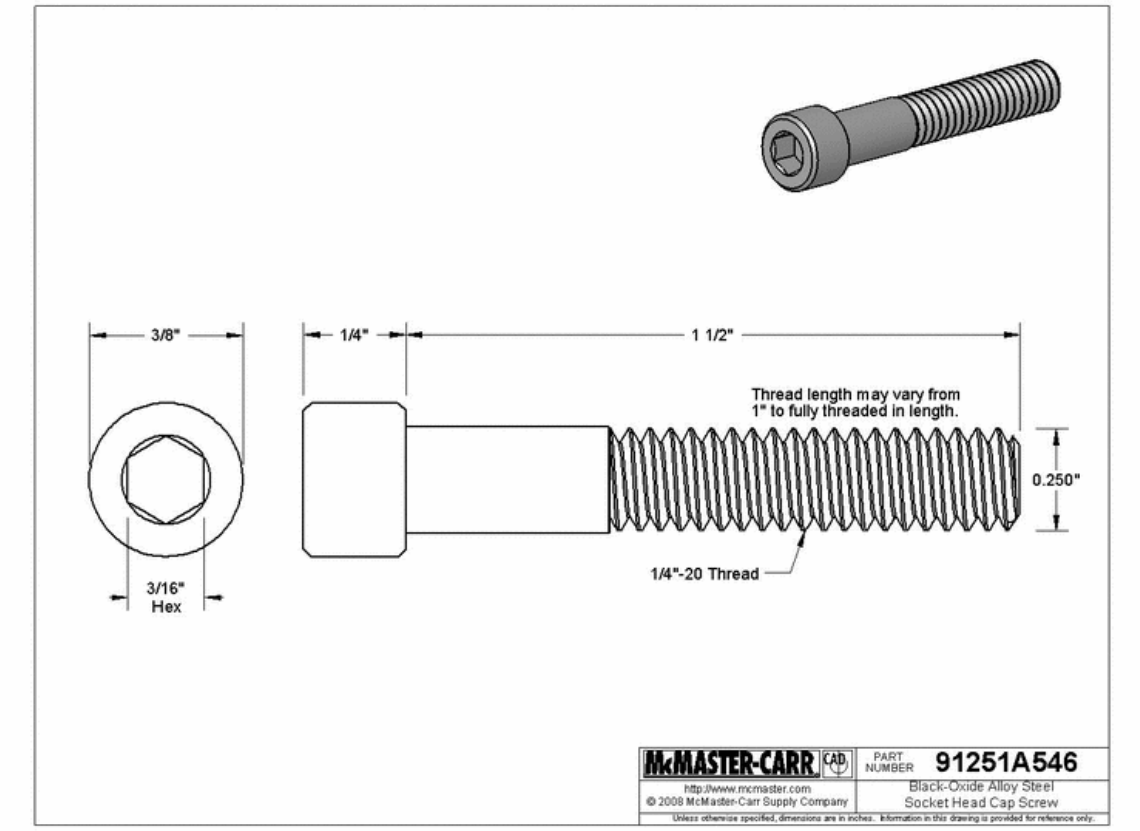

Figure 39 12.7 Millimeter Diameter Bolt (Window Cover) [McMasters]

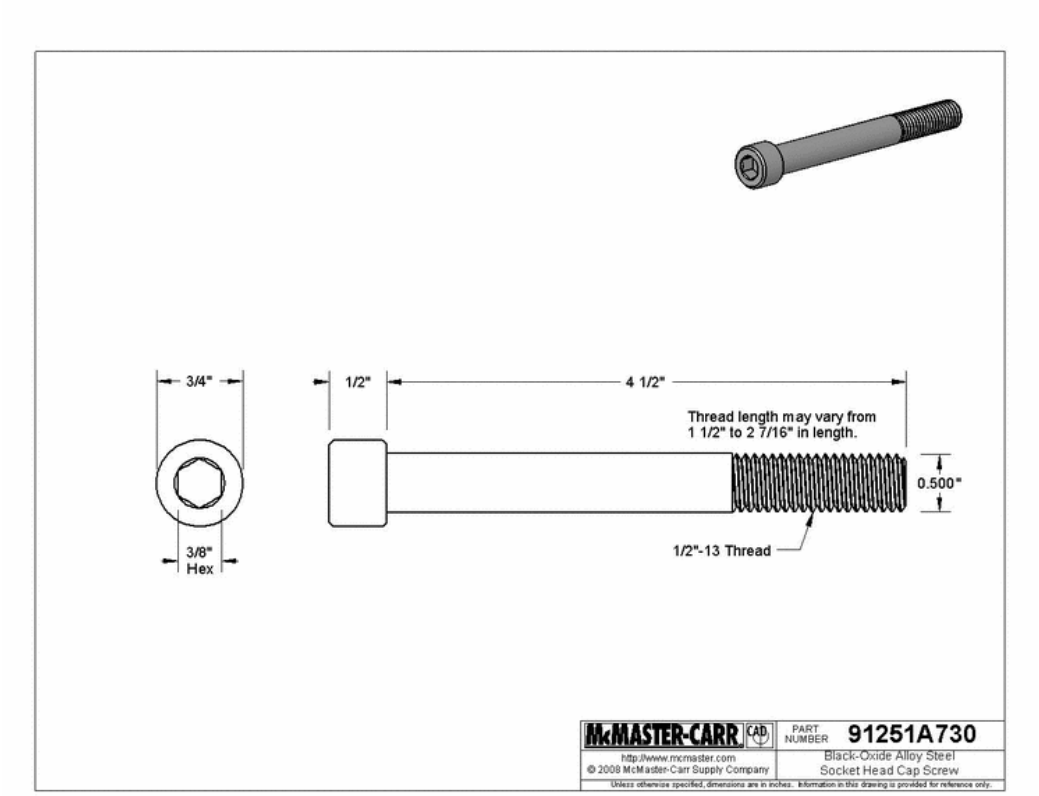

Figure 40 6.35 Millimeter Diameter Bolts (End Cap/ Front Cap) [McMasters]

The stress placed on each bolt was calculated and the results can be seen in Table (8). Due to the material of the bolts and the combustion chamber consisting of different material and having coefficient of thermal expansion different to each other it is then necessary to find the thermal loading in each bolt. The Equation (13) was used to find the thermal load of each bolt and the results can be seen in

$$F_t = \frac{k_j k_b}{k_j + k_b} \Delta T L_b (\propto_j - \propto_b) \tag{13}$$

Table 6 Equation 11 Properties

	Front Cap 12.7 mm Bolt	End Cap 12.7 mm Bolt	Window Cover Bolts 6.35
k_b	$.23 * 10^9\ N/m$	$.23 * 10^9\ N/m$	$.17 * 10^9\ N/m$
k_j	$3.68 * 10^9\ N/m$	$3.68 * 10^9\ N/m$	$1.57 * 10^9\ N/m$

$\propto_j$	$\mathbf{11.6 * 10^{-6}\ /C}$
$\propto_b$	$1.5 * 10^{-5}/\ C$
ΔT	(350-300) K

The torque specification can be seen in Table (8) and were found using Equation (14)

$$T_b\ =\ F_p\ (\ K_b)\ (d) \tag{14}$$

Table 7 Equation 12 Properties

	Front Cap 12.7 mm Bolt	End Cap 12.7 mm Bolt	Window Cover Bolts 6.35
F_p	11495.9 N	11495.9 N	2016 N
K_b	.3	.3	.3

The overall stress of each bolt can be seen in Table (8) showing a maximum stress of 91.11 MPa with a yield point of 1055 MPa for the End Cap and Front Cap Bolts.

Table 8 Bolt Stresses

Application	Bolt Size	Thermal Load	Initial Torque	Tensile Stress	Yield Stress	Safety Factor
End Cap Bolts	12.7 millimeters diameter	.368 MPa	43.8 N m	90.75 MPa	1055 MPa	11.6
Front Cap Bolts	12.7 millimeters diameter	.368 MPa	43.8 N m	90.75 MPa	1055 MPa	11.6
Window Cover Bolts	6.35 millimeters diameter	.936 MPa	3.84 N m	12.2 MPa	1055 MPa	80.3
Instrumentation Port Bolts	6.35 millimeters diameter	.936 MPa	.724 N m	64.5 MPa	1055 MPa	16.1

4.9 TEST MOUNTING

The main purpose of the test mounting facility is hold the combustor in place and prevent it from moving due to the trust created from combustion. The use of Equation (15) (Hill and Peterson 1992) was used to determine the thrust created. With an overall thrust of 1966 N.

$$Trust = \dot{m}_a[(1+f)(u_e) - u] + (P_e - P_a)A_e \quad (15)$$

The use of three by 7.62 cm by 7.62 cm square tubing was used with an inner thickness of 9.52500 millimeters. The material used is A36 due to lost cost, availability, and meeting suitable operating condition found in the FEA. The length and width is 0.8255 meters by 0.7112 meters with the height being 0.7112 meters. The stand is composed of a two tier system with the combustor being held in place by four curvature supports. Two if which connect the end cap and front cap, using 19.05 millimeters diameter bolts, due to the thrust created by the combustor outlet nozzle. The use of removable wheels is used to position the combustor in place and dampers attached to the floor will be used when the combustor is operational. The combustor will be mounted using a two eye bolts attached to the top of the end cap and front cap and a lift will be used to position the combustor in place. The design of the mounting can be seen in Figure 40 while the curvatures used to attach the combustor can be seen in Figure 40.

Figure 41 Test Stand and Combustor

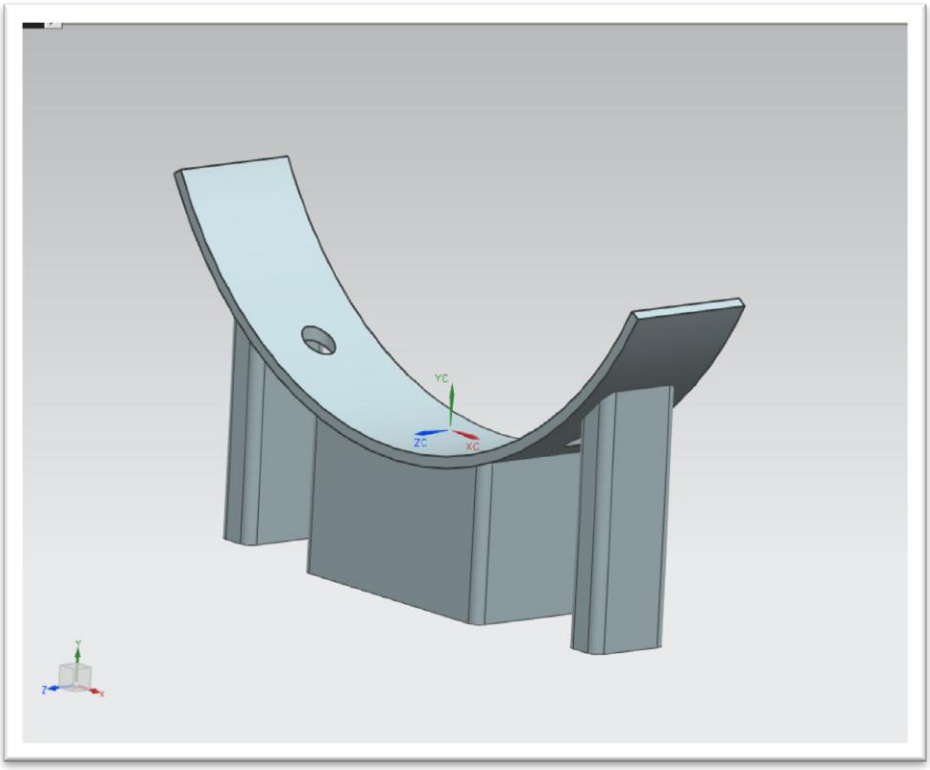

Figure 42 Attachment Curvature

4.10 GASKETS

Gaskets are used throughout the assembly to prevent leaks and in place of any metal to metal or quartz to metal contact. The use of Unifrax high temperature 1600 paper are used with the complete technical properties listed in Appendix D. The maximum use temperature is given as 1873 Kelvin with a maximum shrinkage of 4 %. The paper is made of high purity crystalline alumina fiber stabilized by small amounts of silica providing chemical and thermal stability. [Unifrax].

4.11 MANUFACTURING

After the completed design of the combustor was finalized the manufacturing stage of the project was undertaken. Currently the manufacturing of the presented design continues to be a working

project and ongoing work is needed to make the combustor operational. The current status of the combustor includes the completion of the inlet manifold and testing stand. Also the main chamber has been manufactured and assemble to allow testing using the stainless steel as the main combustion chamber. The current completed manufactured parts can be seen in the Figure 14 and show the inlet manifold, end cap, main chamber, window covers, instrumentation covers, front cap, and testing stand assembled and in its current state. A pressure test has also been conducted to check for any leaks in the combustor.

5. Summary and Conclusions

5.1 CONCLUSION

The main objective of this project was to design an optically accessible high pressure combustor. The following steps were conducted to design and develop the combustor. The adiabatic flame temperature was determined. The wall temperature was found as a function of time and the needed flow rate of H_2O and $N_2$was calculated to maintain the combustor at a safe operable condition. Finite element analysis was conducted on the combustion chamber and included the front cap, main chamber, quartz tube, window covers, quartz windows, and end cap. The design stages of the combustor were also covered and the design description and purpose of each individual component was included. The stress analysis of the bolts was conducted and the FEA and description of the testing stand was also covered.

5.2 FUTURE WORK

The modular design of the combustor incorporates two different testing capabilities. One was the use of a quartz tube acting as the main combustion chamber the other is the removal of the quartz tube and allowing the stainless steel to act as the main chamber. Due to time and cost restraints at this point the combustor can be used only using the latter configuration. If the quartz tube configuration is needed the end cap and front cap can be machined to allow for this assembly. The manufacturing of the nitrogen distributor and end cap nitrogen disk would also be needed for the cooling necessary when using the quartz tube as the main chamber. Also the purchasing of the quartz tube would be necessary.

Before testing the cooling system will need to be implemented. The use of copper cooling coils as shown in Figure (13) would be necessary while the water flow rate needed to cool the

combustor to safe operating conditions can be found in Chapter 3. The need to develop the ignition system will also be needed and the control systems necessary to control the fuel/air, water, nitrogen, and methane will also need to be completed.

5.3 FUTURE TESTING

Once the combustor is completed it would then be possible to conduct experiments to analyze the flame characteristics using a high speed PIV system to determine the effects of fuel composition on flame characteristics particularly in realistic turbine conditions.

Reference

. "AZOM." *Stainless Steel 410*. N.p., 2012. Web. 1 Apr 2012 <http://www.azom.com/article.aspx?ArticleID=970>.

Bidhan, Gildberto , Corona K. Dam, et al. "An Experimental Investigation of Combustion Induced Vortex Breakdown Flashback in a Swirl Stabilized Burner." AIAA. (2011): n. page. Print.

Budynas, Richard. Shigley's mechanical engineering design. Boston: McGraw-Hill, 2008

Compilation of Air Pollutant Emission Factors, AP 42 Volume 1, Fifth Edition, Chapter 3: Stationary Internal Combustion Sources, Section 3.1 Stationary Gas Turbines EPA, Washington DC, April 2000

Department of Engineering Combustion for gas turbines. "High Pressure Combustion Facility." Editorial. Combustion for Gas Turbines. Department of Engineering , 2009. Web. 25 Feb. 2012.<http://www-g.eng.cam.ac.uk/gtcombustion/facilities/index-facilities.html>.

Heraeus, . "TSC Series." . N.p., 02/2009. Web. 2/2012. <www.base-materials.heraeus-quarzglas.com>.

Hill, Philip. Mechanics and thermodynamics of propulsion. Reading, Mass: Addison-Wesley, 1992.

H.J. Tomezak, G. Benelli, L Carrai, D. Cecchini “Investigation of a Gas Turbine Combustor Sytem Fired With Mixtures of Natural Gas and Hydrogen”,

IRVIN, . "UCI COmbustion Laboratory." . N.p., 9/2010. Web. 27 Apr 2012. <http://www.ucicl.uci.edu/2/default.asp&xgt;.\

J.H. Frank, M. F. Miller, M G. Allen “Imaging of Laser-Induced Fluorescence in a High Pressure

Combustor” Physical Science Inc.

J. Sato, K. Konishi, H. Okada, T. Niioka, “Ignition Process of Fuel Spray Injected into High Pressure High Temperature Atmosphere” ,Vol-21, 1988, Symposium (International) On Combustion ,p-695-702

MATWEB." Material Property Data. N.p., 12/2009. Web. 1 Apr 2012.

<http://www.matweb.com/search

National Energy Technology Laboratory

http://www.netl.doe.gov/onsite_research/Facilities/high-pressure.html

Pennsylvania State University, . "Description of PSU’s High Pressure Combustion Lab Capabilities and Projects." . Chemical Propulsion Information Center, n.d. Web. 25 Apr 2012.<http://www.google.com/url?sa=t&rct=j&q=&esrc=s&source=web&cd=2&ved=0CCoQFjAB&url=http://www.hpcl.psu.edu/_notes/CPIAC%20Bulletin.doc&ei=vl2YT_jpKcWL2AWs4M2QBw&usg=AFQjCNGqGNkiMQZjHQQsgj-qIJqQu53jkw&sig2=ie6sdgSSZnQElcI4IMC_zA>.

. "Roymech." Bolt Preloading. N.p., 12/2009. Web. 1 Apr 2012.

<http://www.roymech.co.uk/Useful_Tables/Screws/Preloading.html>.

S.Daniele, P,.Jansohn, K.Boulouchos, “Experimental investigation of lean premixed syngas combustion at gas turbine relevant conditions :lean blow out limits, emissions and turbulent flame speed ”,ASME Turbo Expo,2010.

"The World’s First Industrial Gas Turbine Set ." . ASME, 07/1988. Web. 01/2012.

<http://www.pdfdownload.org/pdf2html/view_online.php?url=http://files.asme.org/asmeorg/Communities/History/Landmarks/12281.pdf>.

Tse.S.D., Zhu.D,LaW.C.K, “Optically accessible high-pressure combustion apparatus”, American Institute of Physics.2004

. "Unifrax." 1600 Paper. N.p., 2008. Web. 1 Apr 2012.<http://www.unifrax.com/web/Audit.nsf/ByUNID/B6AA44CDAD87F72F852579EE0004EA80/$File/1600 Paper EN.pdf>.

US. Department of Energy. Coal Our Most Abundant Fuel". 2011. Web. <http://fossil.energy.gov/education/energylessons/coal/gen_coal.html>.

"

.

Appendix

A. ADIABATIC FLAME TEMPERATURE

Table 9 Heat of Formation at 298 K (kJ/kmol)

CO	-110541
H2	0
O2	0
N2	0
C02	-393546
H20	-241845
CO	-110541

Table 10 Specific Heat 2415 K (kJ/kmol-k)

CO2	61.402
H20	53.511
N2	36.558
CO2	61.402

$$0.7\,CO + 0.3H_2 + 0.5(O_2 + 3.76\,N_2) -> 0.7CO_2 + .03\,H_2O + 1.88\,N_2$$

Assuming a steady flow process with no work done to the system and adiabatic conditions H_P=H_R.

$$\cancel{Q} - \cancel{W} = H_p - H_R$$

$$H_P = H_R$$

First step is to solve for H_R using Equation (14). After H_R is found and by assuming an adiabatic temperature the Cp (Specific Heat) of CO_2, H_2O, and N_2 can be calculated. Using the resulting

adiabatic temperatures and the Cp given it is then possible to plug it into Equation (15) to solve for H_P. This procedure is then repeated until $H_P=H_R$ giving the adiabatic temperature.

$$HR = 0.7(h\_f)_{CO} + 0.3(h_f)_{H_2} + 0.5\left((h_f)_{H_2} + 3.76(h_f)_{N_2}\right) \quad (14)$$

$$HP = 0.7(\left(h_f\right)_{CO_2} + (h_s)) + .03(\left(h_f\right)_{H_2O} + (h_s)) + 1.88(\left(h_f\right)_{N_2} + (h_s)) \quad (15)$$

$$\left(h_f\right) = Heat\ Of\ Formation$$

$$(h_s) = Cp(T_{Ad} - T_\infty) = Sensible\ Entropy$$

B. QUARTZ MATERIAL PROPERTIES (Heraeus 2009)

Technical properties

	TSC-3®	TSC-4	TSC-Synthetic
Mechanical Data			
Density (g/cm³)	2.2	2.2	2.2
Mohs Hardness	5.5 ... 6.5	5.5 ... 6.5	5.5 ... 6.5
Micro Hardness (N/mm²)	8600 ... 9800	8600 ... 9800	8600 ... 9800
Knoop Hardness (N/mm²)	5800 ... 6100	5800 ... 6100	5800 ... 6100
Modulus of elasticity at 20°C (N/mm²)	7.3×10^4	7.3×10^4	7.3×10^4
Modulus of torsion (N/mm²)	3.0×10^4	3.0×10^4	3.0×10^4
Poisson's ratio	0.16	0.16	0.16
Compressive strength (approx.) (N/mm²)	1110	1110	1110
Tensile strength (approx.) (N/mm²)	50	50	50
Bending strength (approx.) (N/mm²)	65	65	65
Torsional strength (approx.) (N/mm²)	30	30	30
Sound velocity (m/s)	5700	5700	5700
Thermal Data			
Softening temperature (°C)	1730	1730	1730
Annealing temperature (°C)	1200	1200	1200
Strain temperature (°C)	1080	1080	1080
Max. working temperature continuous (°C)	1050	1050	1050
short-term (°C)	1350	1350	1350

	TSC-3®	TSC-4	TSC-Synthetic
Mean specific heat (J/kg*K)			
0 ... 100°C	772	772	772
0 ... 500°C	964	964	964
0 ... 900°C	1052	1052	1052
Heat conductivity (W/m*K)			
20°C	1.38	1.38	1.38
100°C	1.47	1.47	1.47
200°C	1.55	1.55	1.55
300°C	1.67	1.67	1.67
400°C	1.84	1.84	1.84
950°C	2.68	2.68	2.68
Mean expansion coefficient (K^{-1})			
0 ... 100°C	5.1×10^{-7}	5.1×10^{-7}	5.1×10^{-7}
0 ... 200°C	5.8×10^{-7}	5.8×10^{-7}	5.8×10^{-7}
0 ... 300°C	5.9×10^{-7}	5.9×10^{-7}	5.9×10^{-7}
0 ... 600°C	5.4×10^{-7}	5.4×10^{-7}	5.4×10^{-7}
0 ... 900°C	4.8×10^{-7}	4.8×10^{-7}	4.8×10^{-7}
-50 ... 0°C	2.7×10^{-7}	2.7×10^{-7}	2.7×10^{-7}

Typical Transmission Spectrum (including Fresnel reflection losses)

Sample thickness: 10mm

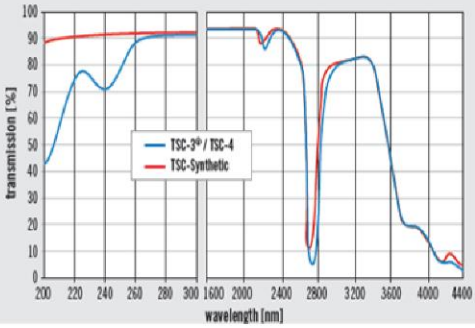

Electric Data

	TSC-3®	TSC-4	TSC-Synthetic
Electrical resistivity in Ω x m			
20°C	10^{15}	10^{16}	10^{16}
400°C	10^{10}	10^{10}	10^{10}
800°C	6.3×10^6	6.3×10^6	6.3×10^6
1200°C	51.3×10^5	51.3×10^5	51.3×10^5
Dielectric strength in KV/mm (sample thickness ≥ 5 mm)			
20°C	25 ... 40	25 ... 40	25 ... 40
500°C	4 ... 5	4 ... 5	4 ... 5
Dielectric loss angle (tg δ)			
1kHZ	5.0×10^{-4}	5.0×10^{-4}	5.0×10^{-4}
1MHz	1.0×10^{-4}	1.0×10^{-4}	1.0×10^{-4}
3×10^{10} Hz	4.0×10^{-4}	4.0×10^{-4}	4.0×10^{-4}
Dielectric constant (ε)			
20°C 0 ... 10^2 Hz	3.70	3.70	3.70
23°C 9 ... 10^9 Hz	3.77	3.77	3.77
23°C 3 ... 10^{10} Hz	3.81	3.81	3.81

HQS-BM TSC 02.2009/V1.0_EA.indd

The data given here is correct at February 2009 and is subject to change.

C. CURRENT PART DRAFTINGS

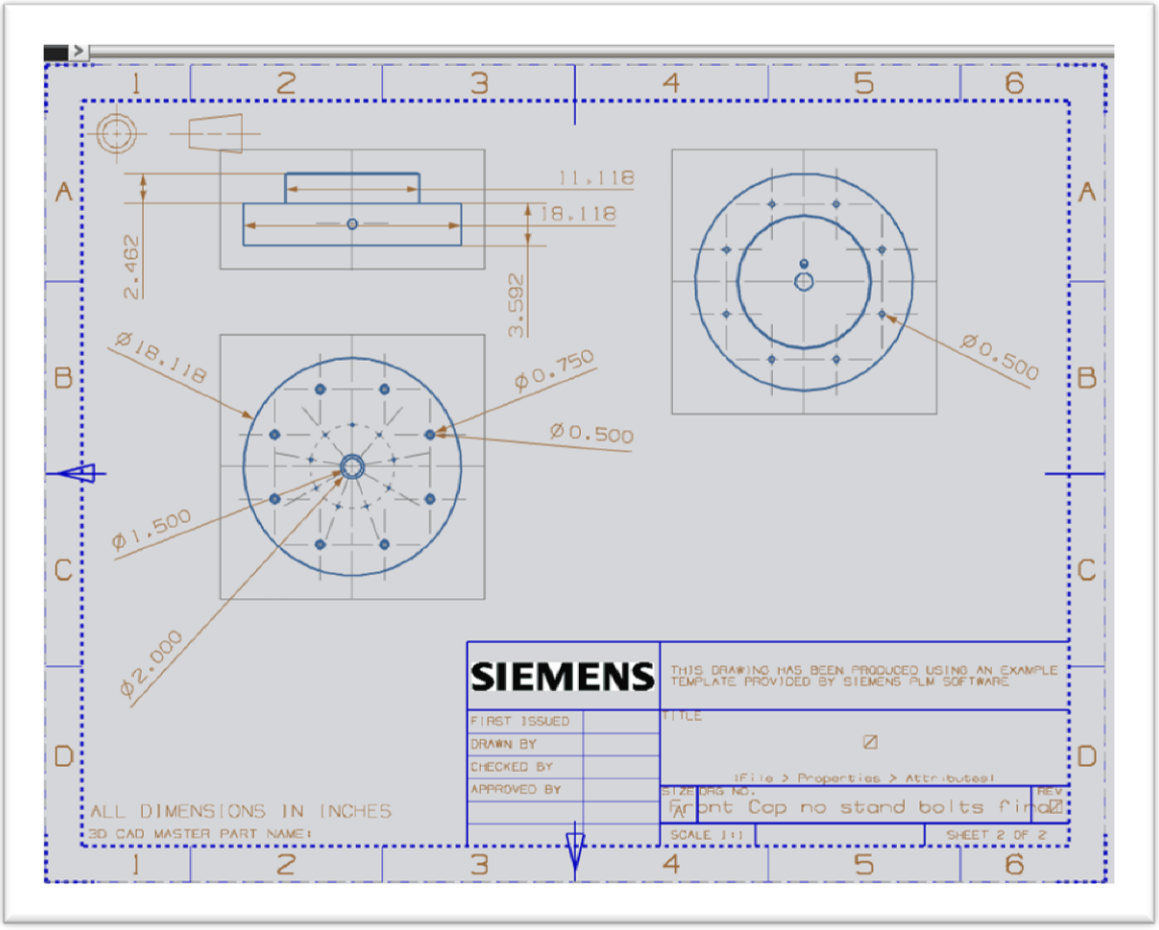

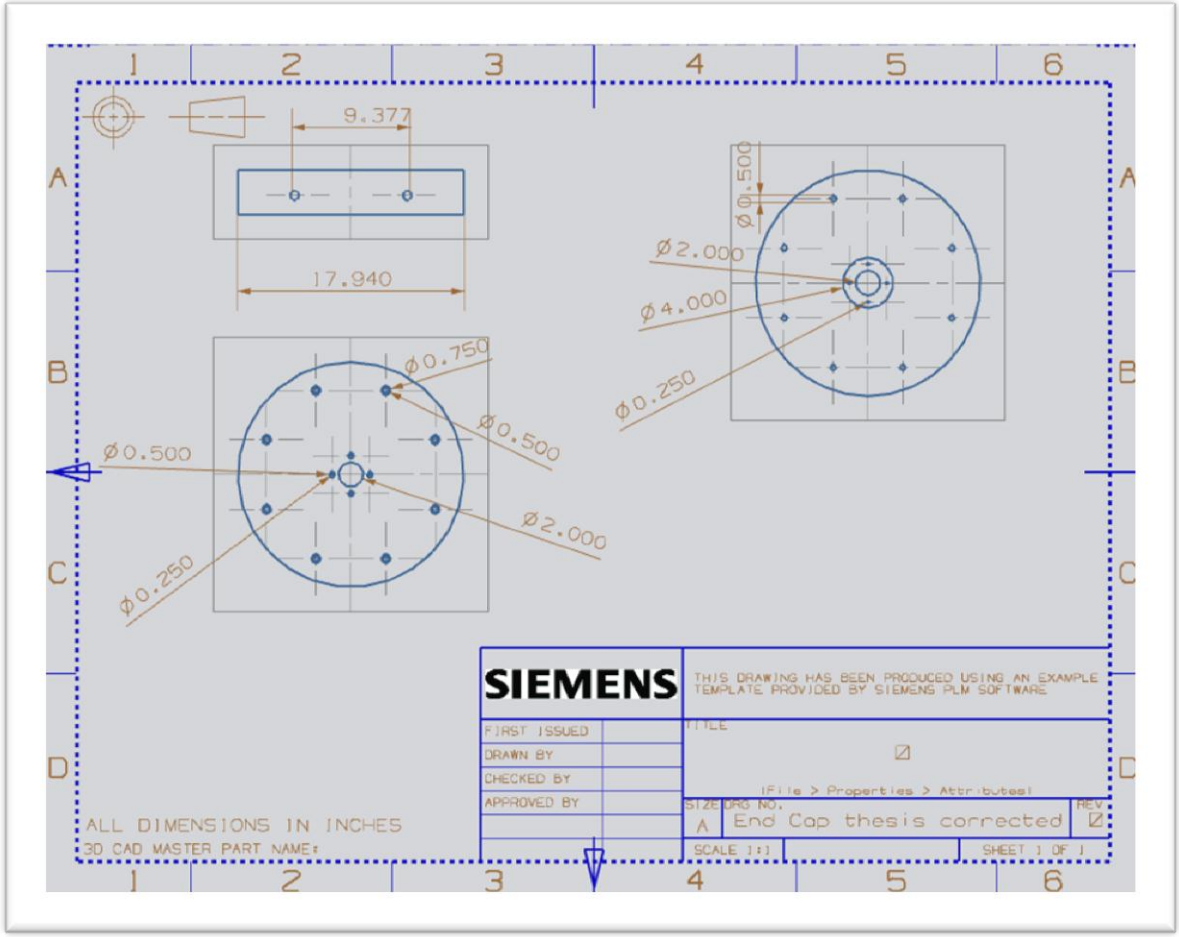
9.377
17.940
Ø0.500
Ø2.000
Ø4.000
Ø0.250
Ø0.750
Ø0.500
Ø0.500
Ø2.000
Ø0.250
SIEMENS
THIS DRAWING HAS BEEN PRODUCED USING AN EXAMPLE TEMPLATE PROVIDED BY SIEMENS PLM SOFTWARE
FIRST ISSUED
DRAWN BY
CHECKED BY
APPROVED BY
TITLE
[File > Properties > Attributes]
SIZE
A
DRG NO.
End Cap thesis corrected
REV
SCALE 1:1
SHEET 1 OF 1
ALL DIMENSIONS IN INCHES
3D CAD MASTER PART NAME:

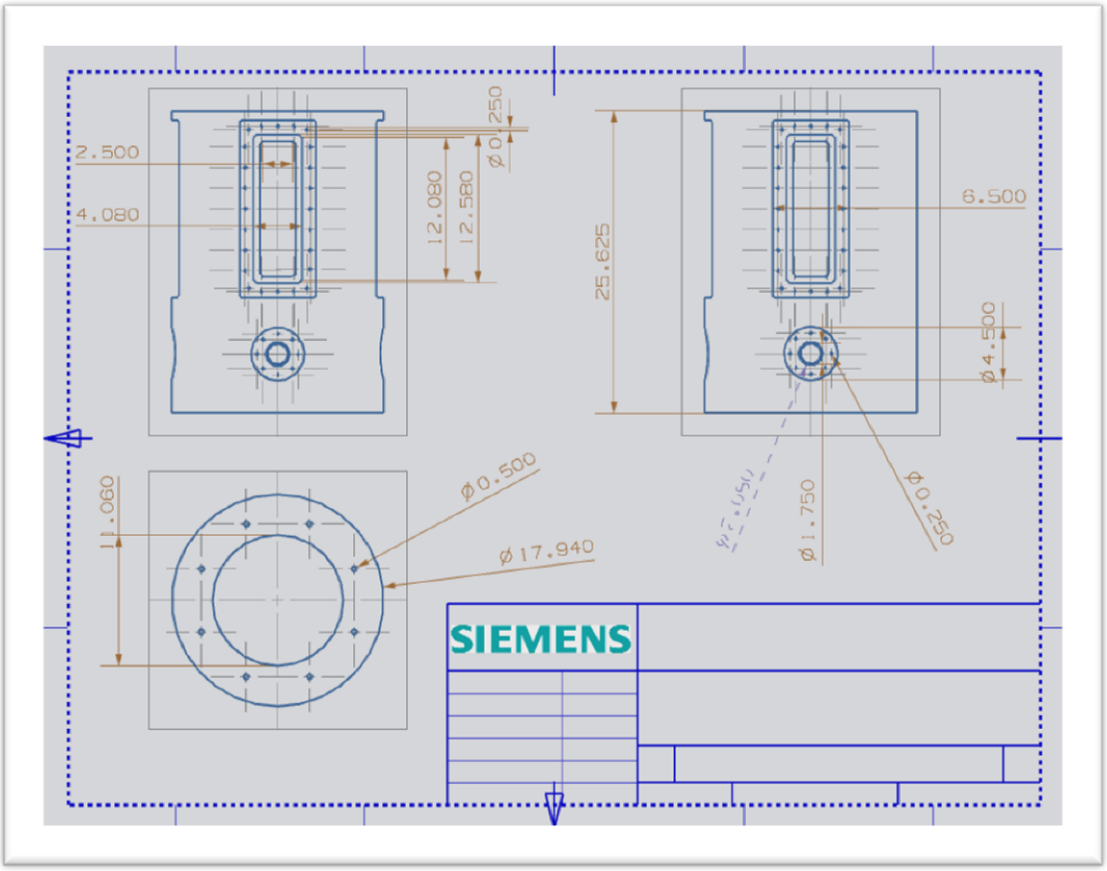
2.500
4.080
12.080
12.580
Ø0.250
25.625
6.500
Ø4.500
11.060
Ø0.500
Ø17.940
Ø1.750
Ø0.250
SIEMENS

D. GASKET (Unifrax)

1600 Paper

TYPICAL PRODUCT PARAMETERS

	1600 Paper
Typical Chemical Analysis (fibre wt. %)	
Al_2O_3	>90.0
SiO_2	<8.0
Trace	<2.0
Physical Properties	
Colour	White
Product Density (kg/m^3)	140 - 200
Classification Temperature (°C) *	1600
Loss on Ignition (wt. %)	<7.0
Thermal Conductivity (W/mK)	
Mean Temp.	
600 °C	0.16
800 °C	0.20
1000 °C	0.24
Permanent Linear Shrinkage (%) 24 Hour Soak	
1600 °C	<4.0

*Classification Temperature is not a definition of the operational limit of these products, especially when long term physical or dimensional stability is a factor. For certain applications continuous use temperature limits may be significantly reduced. For assistance or clarification please contact your nearest Unifrax Engineering office. Where appropriate Physical Properties data measured according to EN 1094-1.

AVAILABILITY

Thickness (mm)	1600 Paper	Roll Length (m)	
	Roll Width (mm)	500	1000
1	✓	10	10
2	✓	10	10
3	✓	10	10

Other thicknesses / sizes may be available on request subject to minimum order requirements.

E. COOLING CALCULATIONS

H20 Ice Water			
Total Heat Removed	388.32	KW	
			Boiling Point 370
Cp	4.19	KJ/Kg K	K
DT	77.00	K	350-273
Mass Flow Rate	1.20	Kg/S	
Mass Flow Rate	1.20	Kg/s	
1 Liter= 1 Kg	1.20	L/s	
1Liter=.26417 Gallon	0.32	Gallons/s	
	19.09	Gallons/m	
	1145.60	Gallons/Hour	

Ethylene glycol 100%			
Total Heat Removed	388.32	KW	
Cp	2.80	KJ/Kg K	Boiling Point 470
DT	77.00	K	350-273 K
Mass Flow Rate	1.80	Kg/S	
Mass Flow Rate	1.80	Kg/s	
Kg=Lt	1.62	L/s	
1Liter=.26417 Gallon	0.43	Gallons/s	
	25.72	Gallons/m	
	1543.14	Gallons/Hour	

Ethylene glycol 30%			
Total Heat Removed	388.32	KW	
Cp	3.33	KJ/Kg K	
DT	77.00	K	
Mass Flow Rate	1.52	Kg/S	Boiling Point 377
			350-273 K
Mass Flow Rate	1.52	Kg/s	
Kg=Lt	1.37	L/s	
1Liter=.26417 Gallon	0.36	Gallons/s	
	21.66	Gallons/m	
	1299.48	Gallons/Hour	

$$\frac{\cancel{P_1}}{\cancel{\gamma}} + z_1 + \frac{\cancel{v_1^2}}{\cancel{2g}} + h_A - h_L = \frac{\cancel{P_2}}{\cancel{\gamma}} + z_2 + \frac{v_2^2}{2g}$$

Assuming atmospheric conditions in tank and exit. v_1 is assumed to be approximate zero.

$$h_A = z_2 - z_1 + h_L + \frac{v_2^2}{2g}$$

$$h_A = total\ head$$

$$h_L = H1 + H2 + H3 + H4 + H5 + H6 + H7$$

Q=Volumetric Flow Rate	0.001	m^3/s	
Mass Flow Rate	1.210	Kg/s	
Density	998.200	Kg/m^3	
Length	10.000	m	
Pipe Diameter	0.038	m	
Area 1.5 in Pipe	0.001	m^2	
Velocity 1.5 in	1.063	m/s	
Area	0.000	m^2	
Velocity .25 in	0.957	m/s	Assuming 40 Line Distribution Around Combustion Chamber
(.25) V^2/2g	0.047	m	
(1.5 in) V^2/2g	0.058	m	
Z2	1.200	m	
Z1	0.000	m	
Entrance Loss H1	0.029	m	Assuming Square Edge K=.5
Friction Line H2 1.5 in D	0.318	m	f Friction Factor=.021
Friction Line H3 .25 in D	0.711	m	f friction factor=.029
Valve Loss H4	0.412	m	Assuming Glove Valve K=340*f
Flow Through Branch H5	6.499	m	Flow Through Branch K=60* f 80 total
90 Elbow H6	0.145	m	Elbow K=30*f 4 total
Exit loss H7	0.058	m	K=1
Total Head Loss HA	9.371	m	
	30.736	Ft	
y	9792.342		

Power of Pump	145.368	W
	0.195	HP

F. FLUENT ANALYSIS

Temperature: Outlet View

Simulation of the Flow Field of Water over the Stainless Steel Chamber Assuming the Use of a Cooling Jacket

Mass Flow Rate 1.21 Kg/s

Max Temperature= 525 K

Constant Heat Flux= 897 W/m^2

500 KW

Inlet View

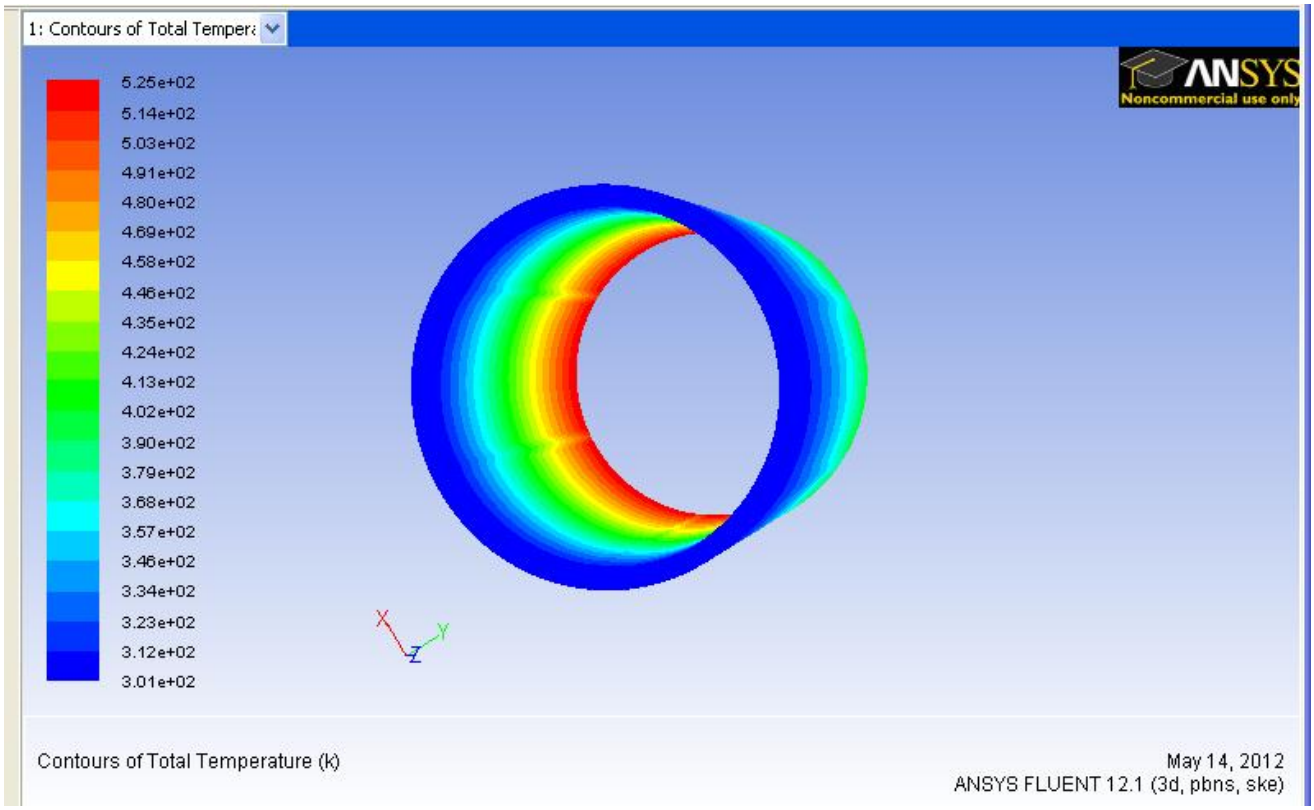

Outlet View

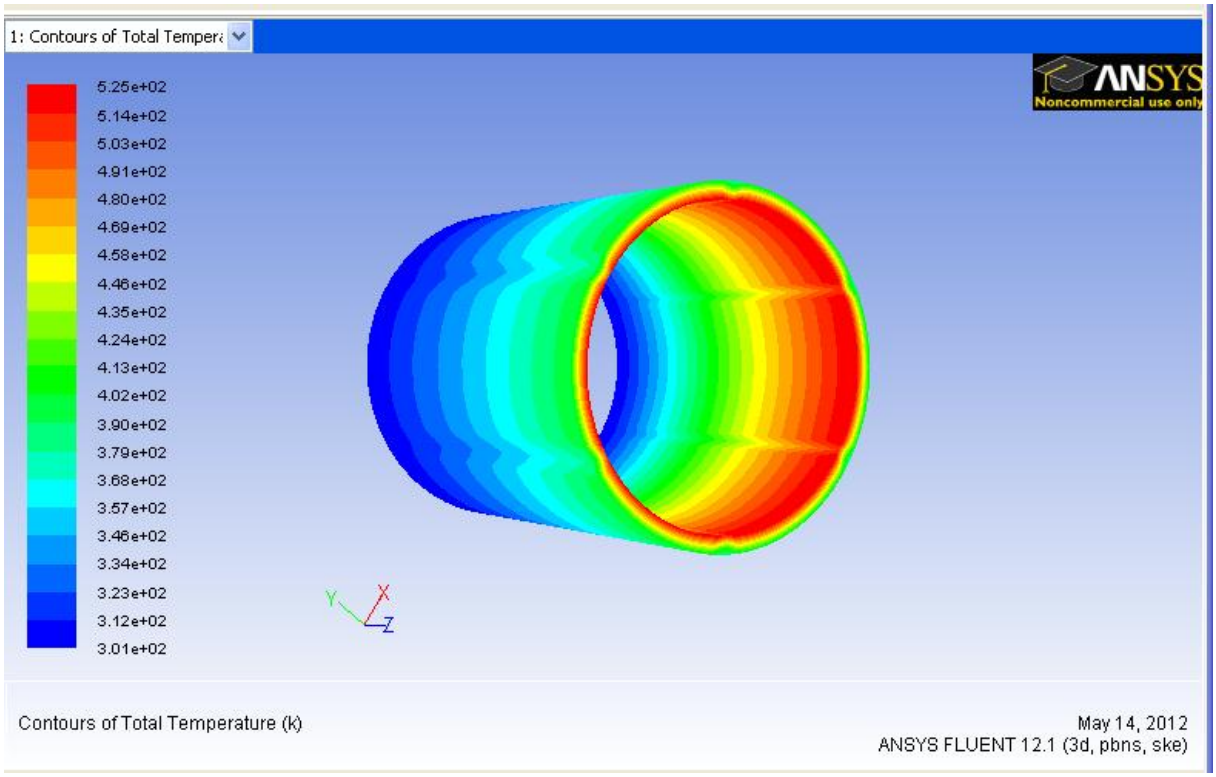

Velocity:

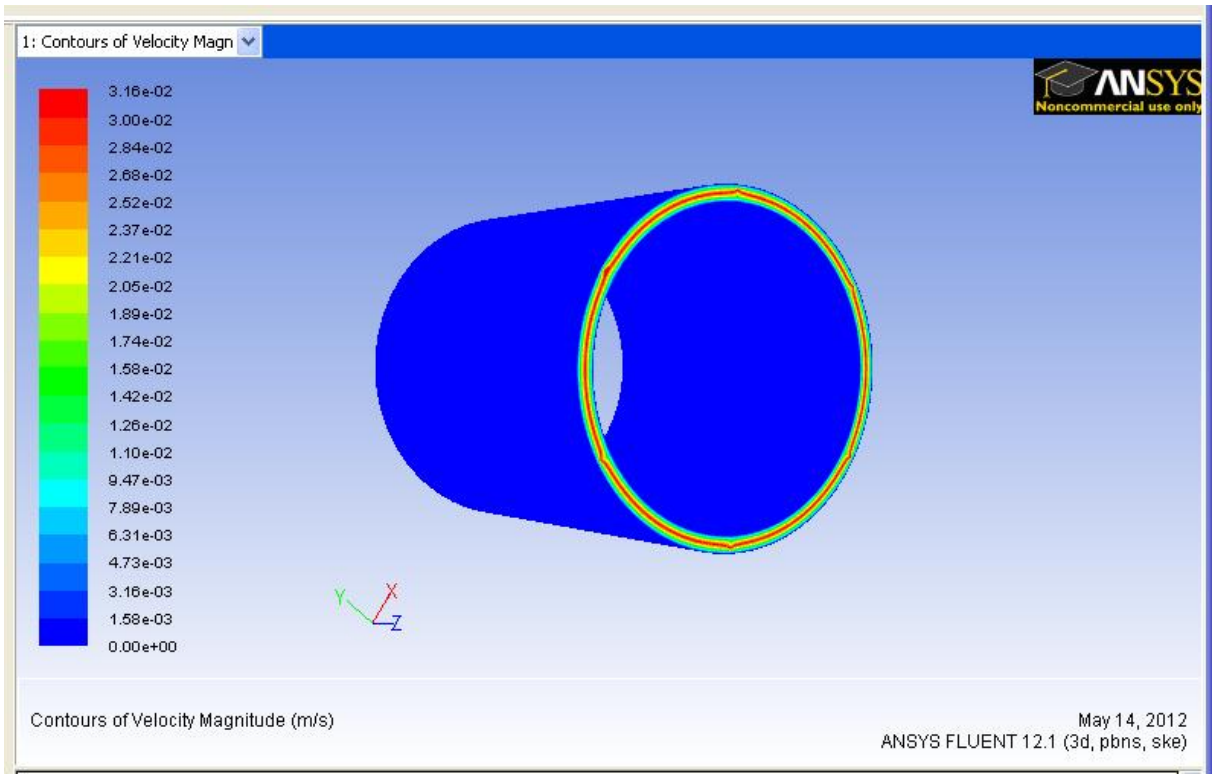

Temperature: Outlet View

Simulation of the Flow Field of Water over the Stainless Steel Chamber Assuming the Use of a Cooling Jacket

Mass Flow Rate 1.21 Kg/s

Max Temperature= 445 K

Constant Heat Flux= 687000 W/m^2

383 KW

Initial Temperature 273 K of Water

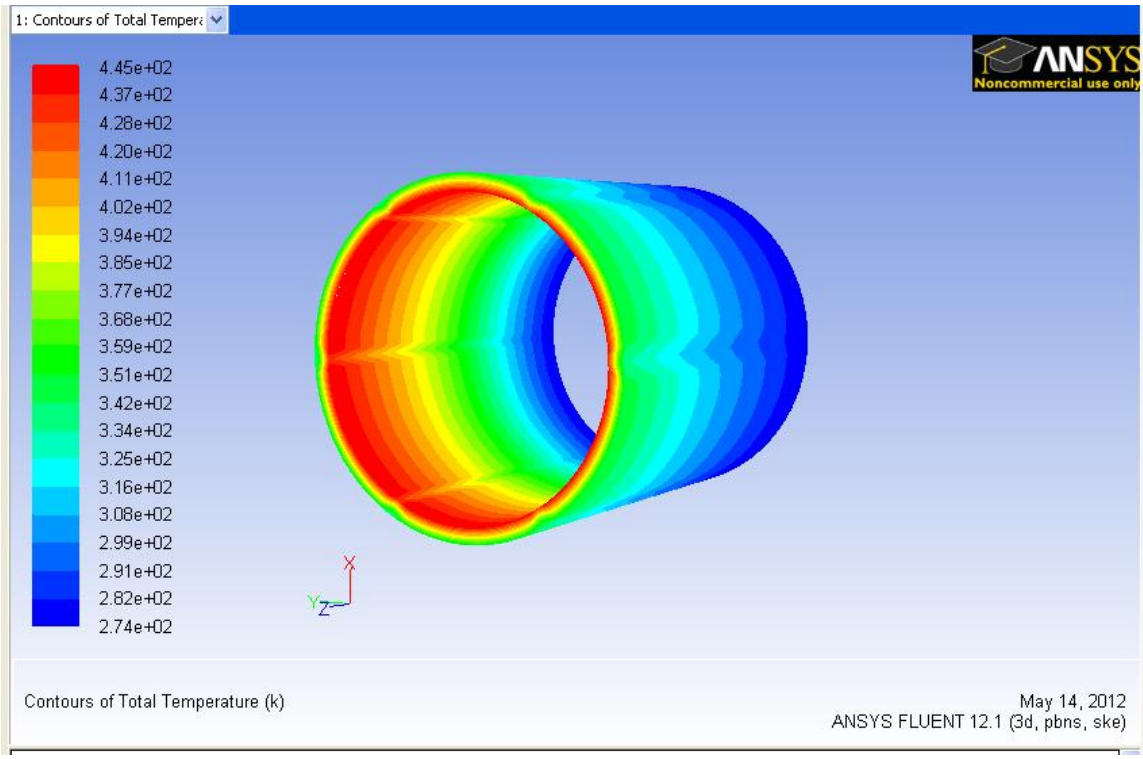

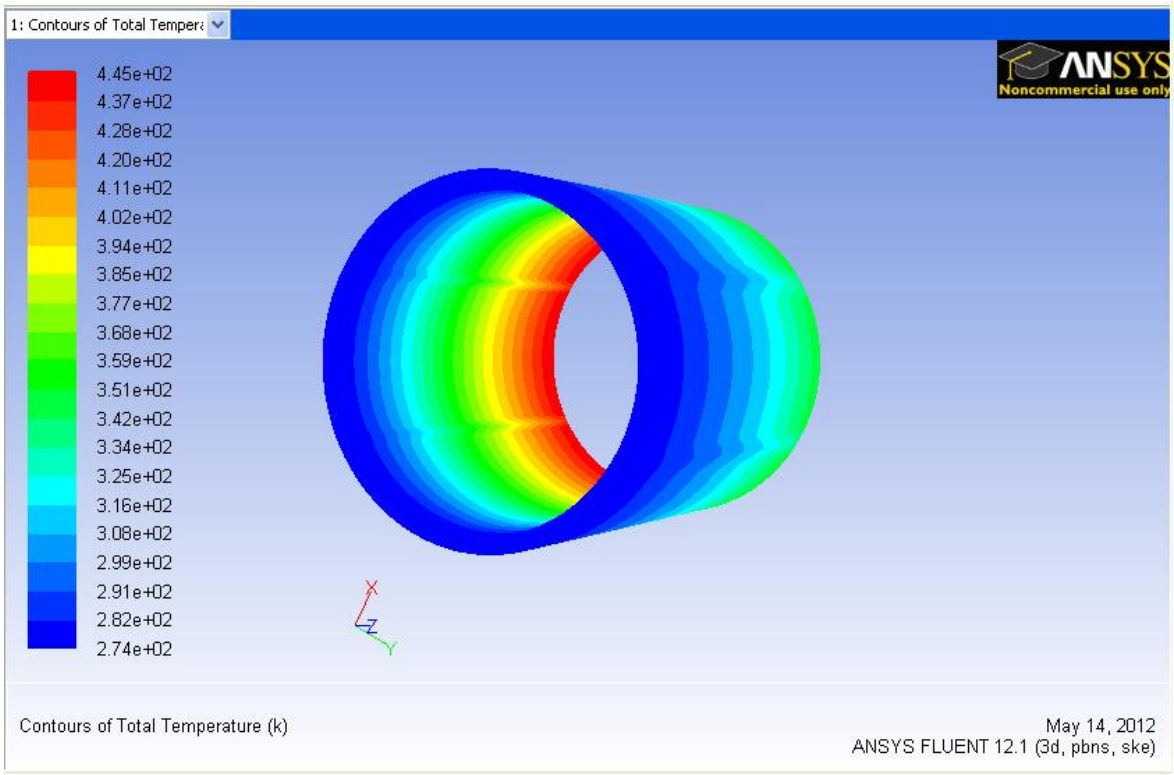
1: Contours of Temper
4.45e+02
4.37e+02
4.28e+02
4.20e+02
4.11e+02
4.02e+02
3.94e+02
3.85e+02
3.77e+02
3.68e+02
3.59e+02
3.51e+02
3.42e+02
3.34e+02
3.25e+02
3.16e+02
3.08e+02
2.99e+02
2.91e+02
2.82e+02
2.74e+02
ANSYS
Noncommercial use only
Contours of Total Temperature (k)
May 14, 2012
ANSYS FLUENT 12.1 (3d, pbns, ske)

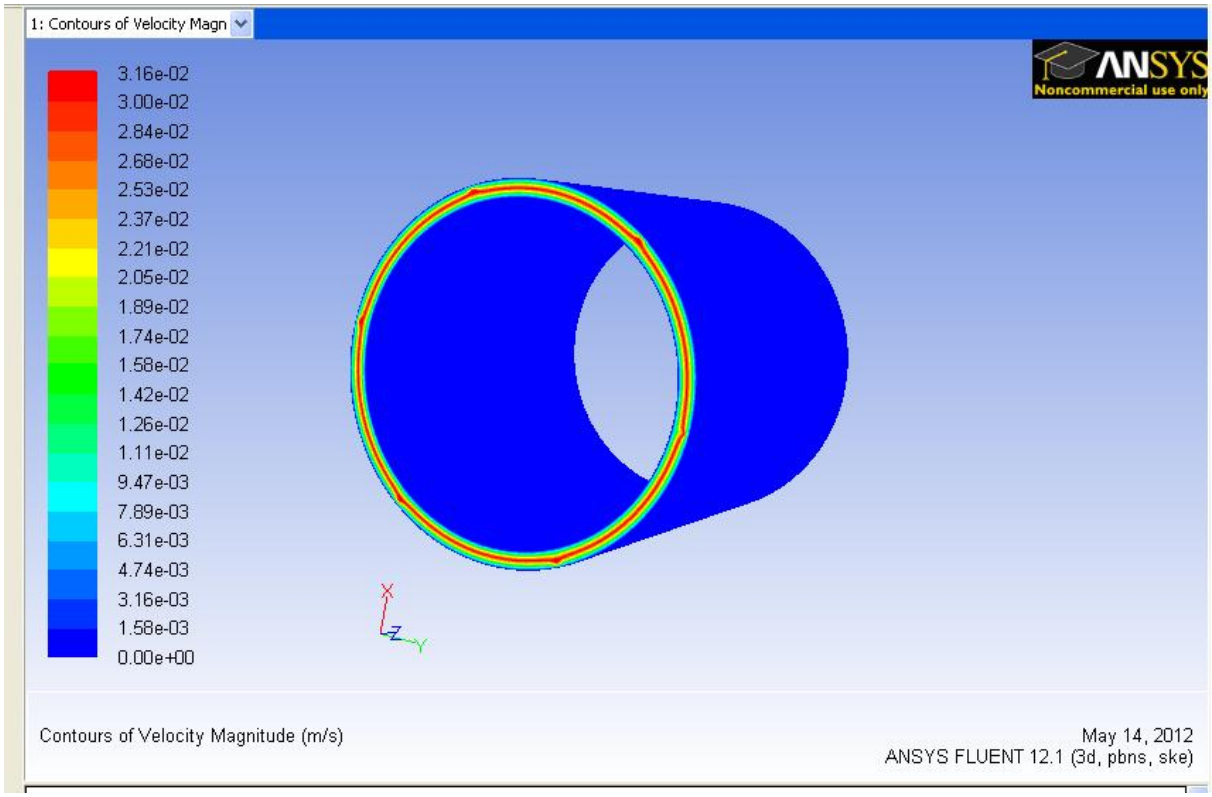
1: Contours of Velocity Magn
3.16e-02
3.00e-02
2.84e-02
2.68e-02
2.53e-02
2.37e-02
2.21e-02
2.05e-02
1.89e-02
1.74e-02
1.58e-02
1.42e-02
1.26e-02
1.11e-02
9.47e-03
7.89e-03
6.31e-03
4.74e-03
3.16e-03
1.58e-03
0.00e+00
ANSYS
Noncommercial use only
Contours of Velocity Magnitude (m/s)
May 14, 2012
ANSYS FLUENT 12.1 (3d, pbns, ske)

Simulation of the Flow Field of Water over the Stainless Steel Chamber Assuming the Use of a Cooling Jacket

Mass Flow Rate 2.5 Kg/s

Max Temperature= 412 K

Constant Heat Flux= 897 W/m^2

500 KW

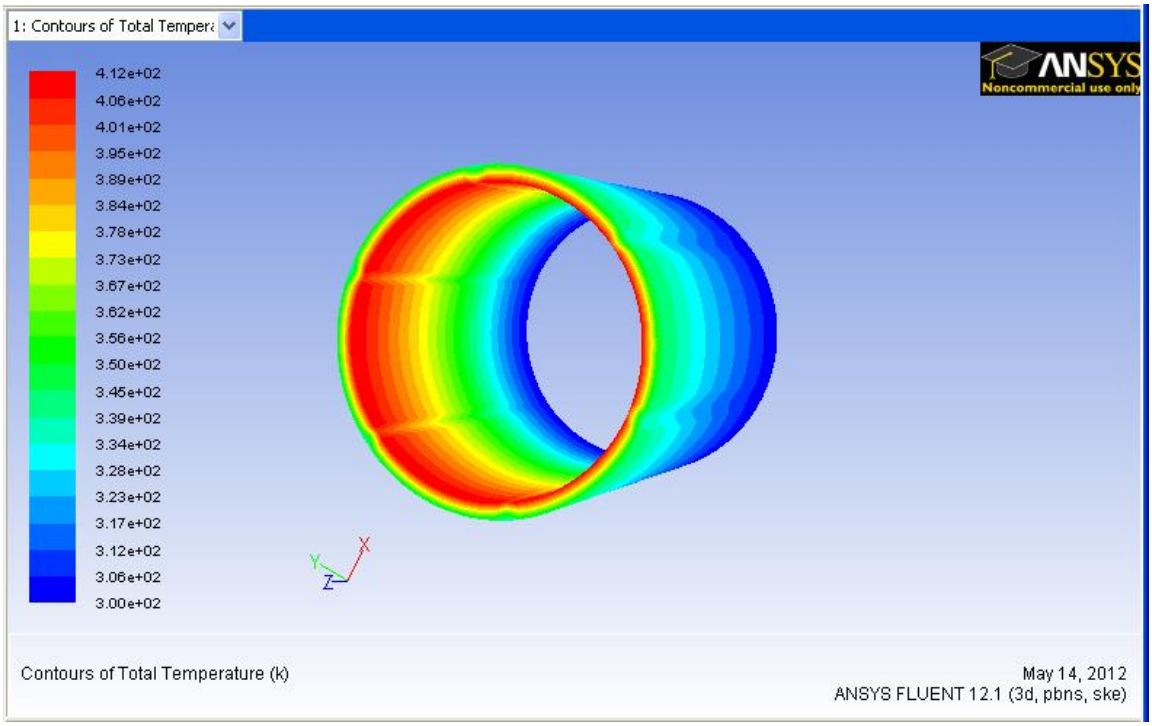

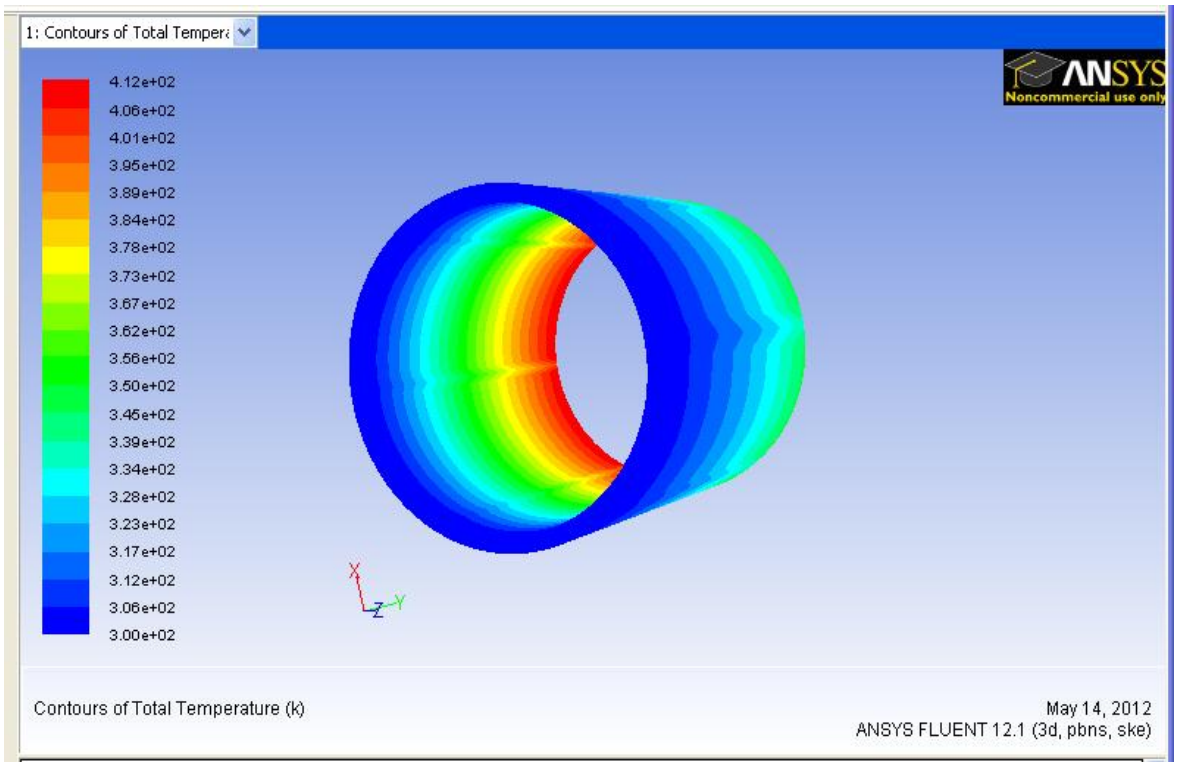

Velocity:

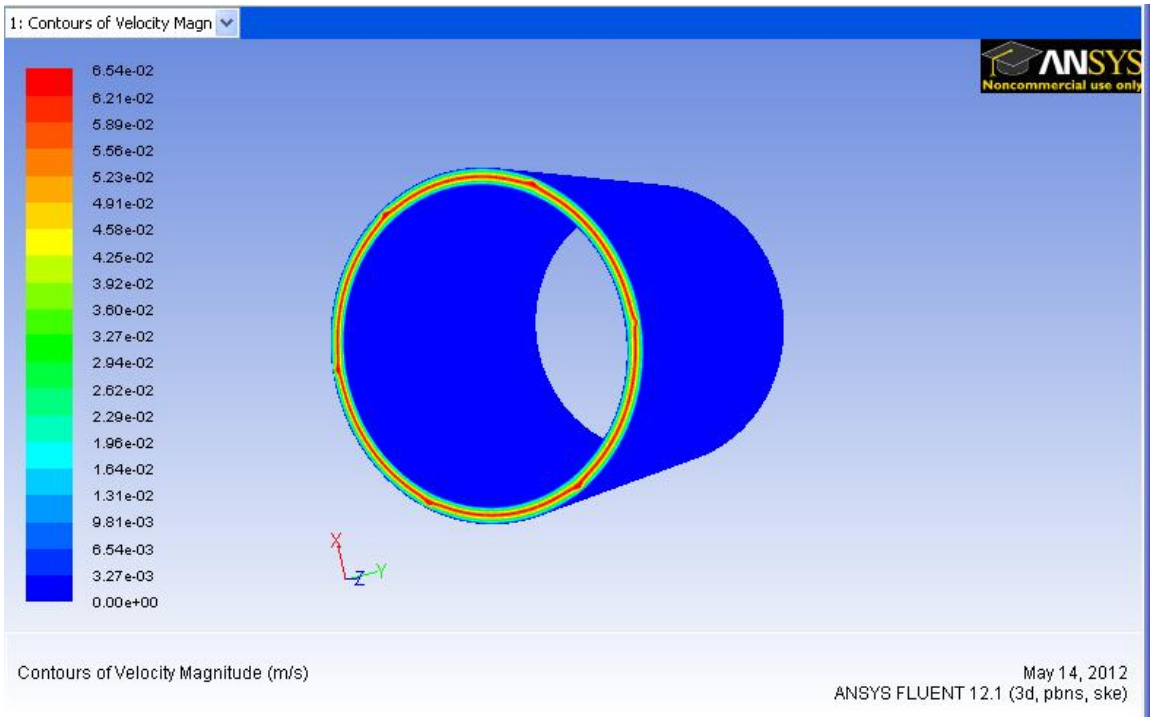

Temperature: Outlet View

Simulation of the Flow Field of Water over the Stainless Steel Chamber Assuming the Use of a Cooling Jacket

Mass Flow Rate 2.5 Kg/s

Max Temperature= 386 K

Heat Flux= 687000 W/m^2

383 KW

Inlet Vie:

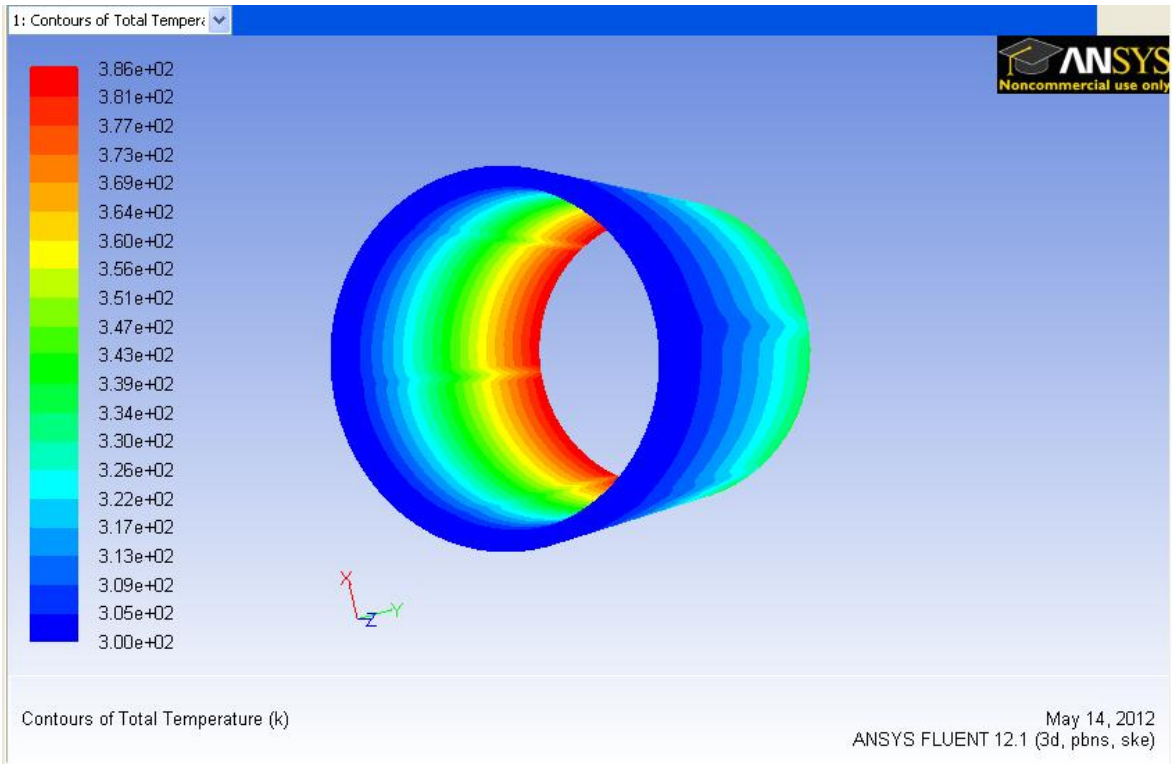

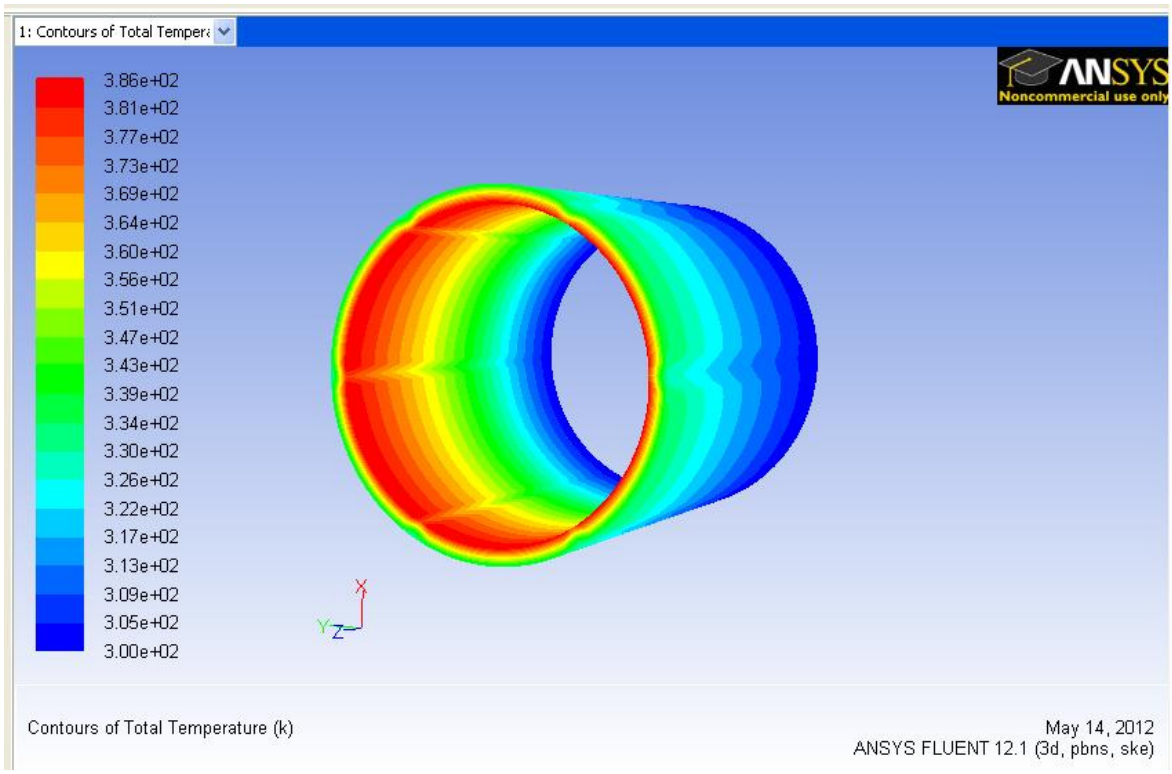
1: Contours of Tempera
3.86e+02
3.81e+02
3.77e+02
3.73e+02
3.69e+02
3.64e+02
3.60e+02
3.56e+02
3.51e+02
3.47e+02
3.43e+02
3.39e+02
3.34e+02
3.30e+02
3.26e+02
3.22e+02
3.17e+02
3.13e+02
3.09e+02
3.05e+02
3.00e+02
ANSYS
Noncommercial use only
Contours of Total Temperature (k)
May 14, 2012
ANSYS FLUENT 12.1 (3d, pbns, ske)

Velocity:

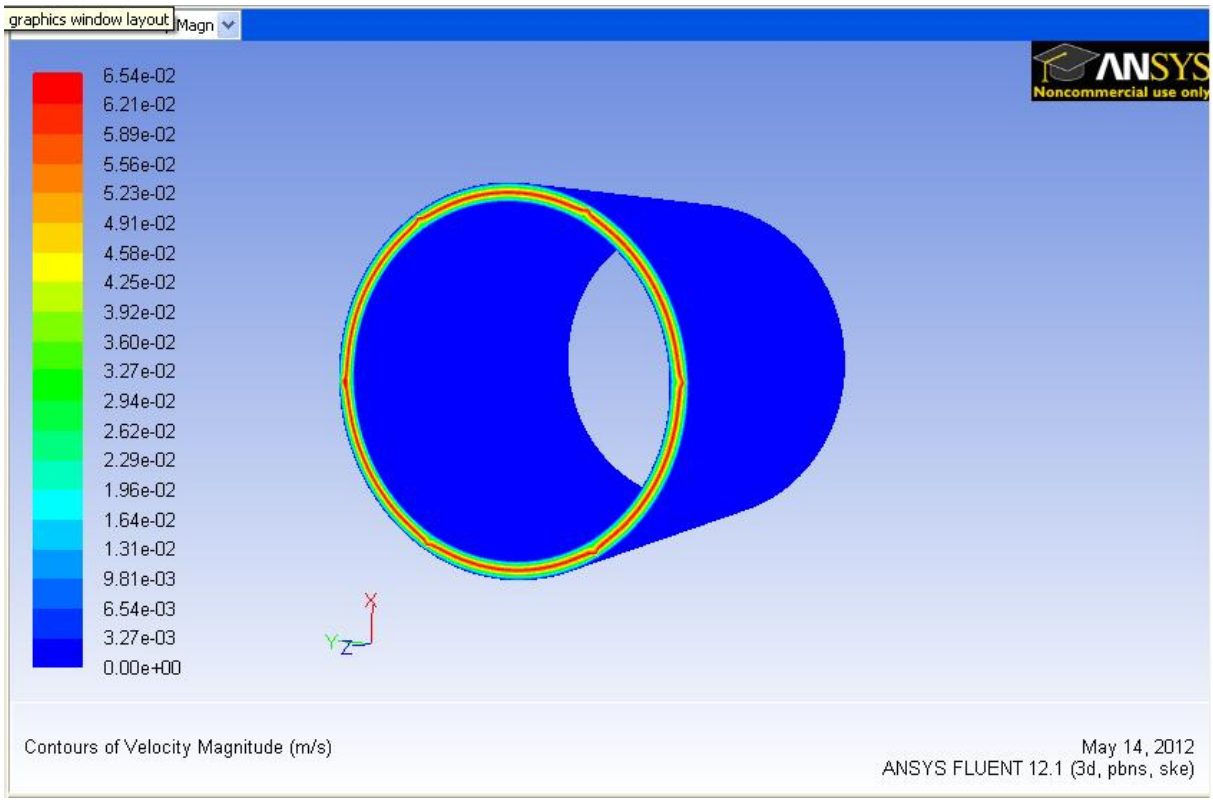
graphics window layout
Magn
6.54e-02
6.21e-02
5.89e-02
5.56e-02
5.23e-02
4.91e-02
4.58e-02
4.25e-02
3.92e-02
3.60e-02
3.27e-02
2.94e-02
2.62e-02
2.29e-02
1.96e-02
1.64e-02
1.31e-02
9.81e-03
6.54e-03
3.27e-03
0.00e+00
ANSYS
Noncommercial use only
Contours of Velocity Magnitude (m/s)
May 14, 2012
ANSYS FLUENT 12.1 (3d, pbns, ske)

Simulation of the Flow Field of Water over the Stainless Steel Chamber Assuming the Use of a Cooling Jacket

Mass Flow Rate 2.8 Kg/s

Max Temperature= 350 K

Heat Flux= 687000 W/m^2

383 KW

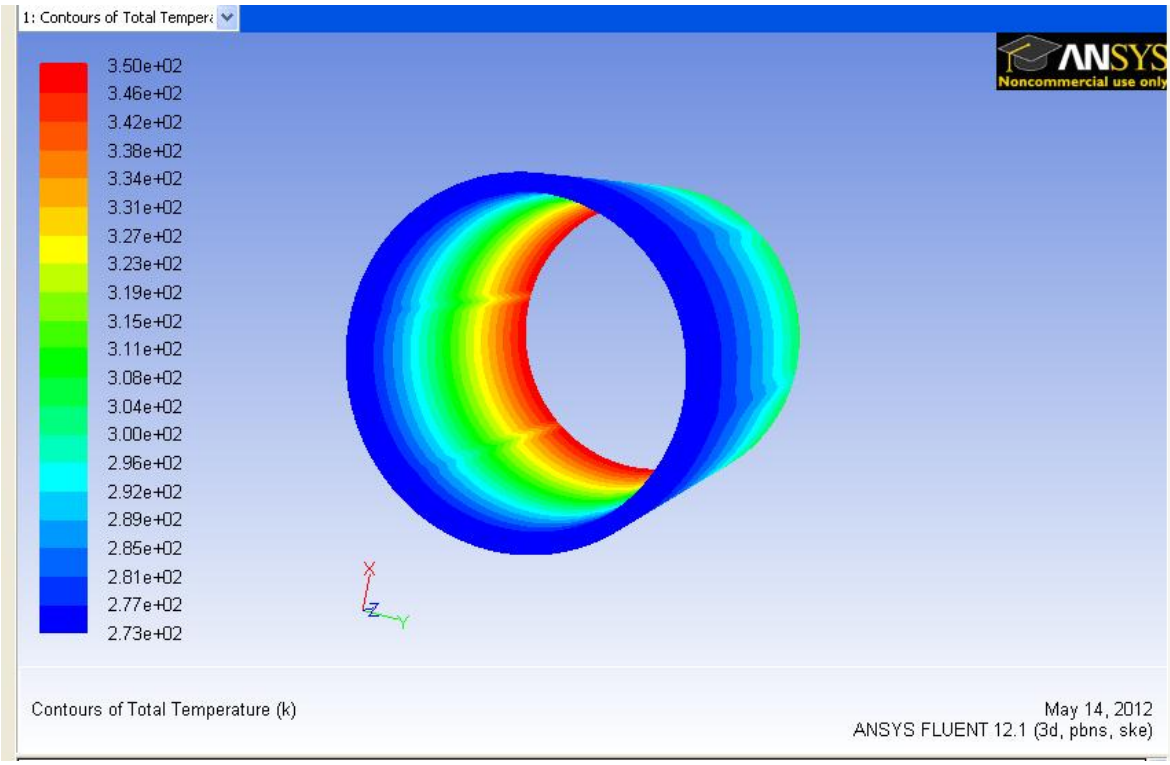

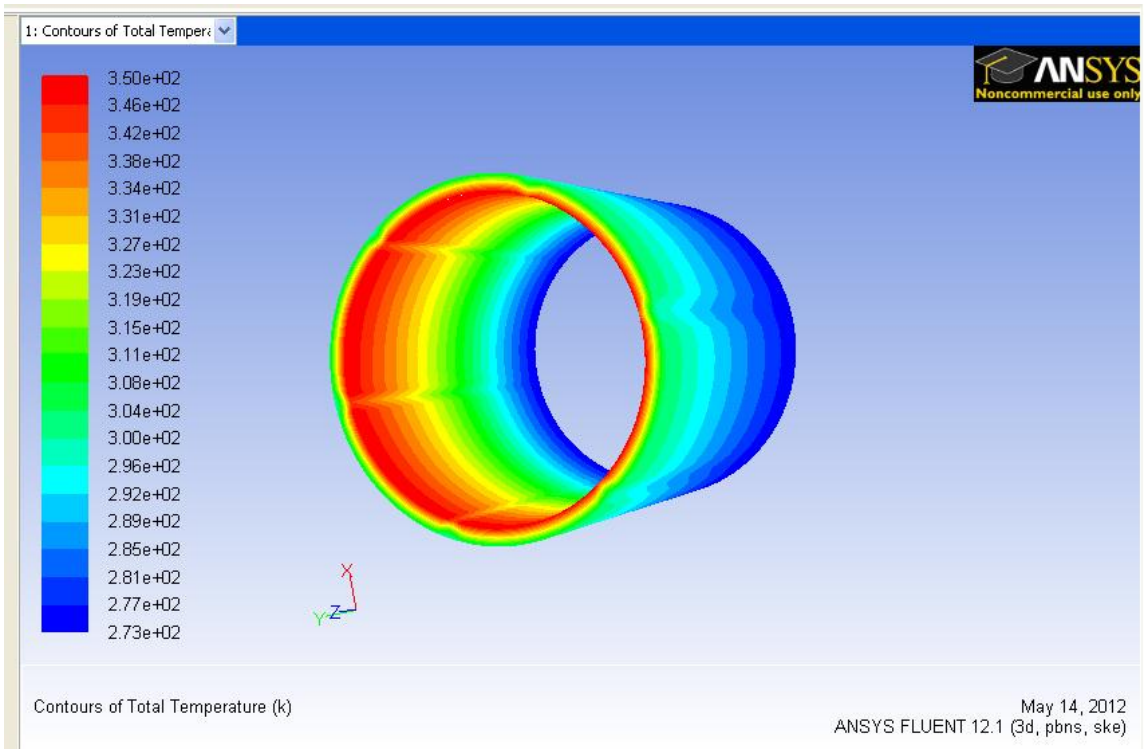
1: Contours of Temper
3.50e+02
3.46e+02
3.42e+02
3.38e+02
3.34e+02
3.31e+02
3.27e+02
3.23e+02
3.19e+02
3.15e+02
3.11e+02
3.08e+02
3.04e+02
3.00e+02
2.96e+02
2.92e+02
2.89e+02
2.85e+02
2.81e+02
2.77e+02
2.73e+02
ANSYS
Noncommercial use only
Contours of Total Temperature (k)
May 14, 2012
ANSYS FLUENT 12.1 (3d, pbns, ske)

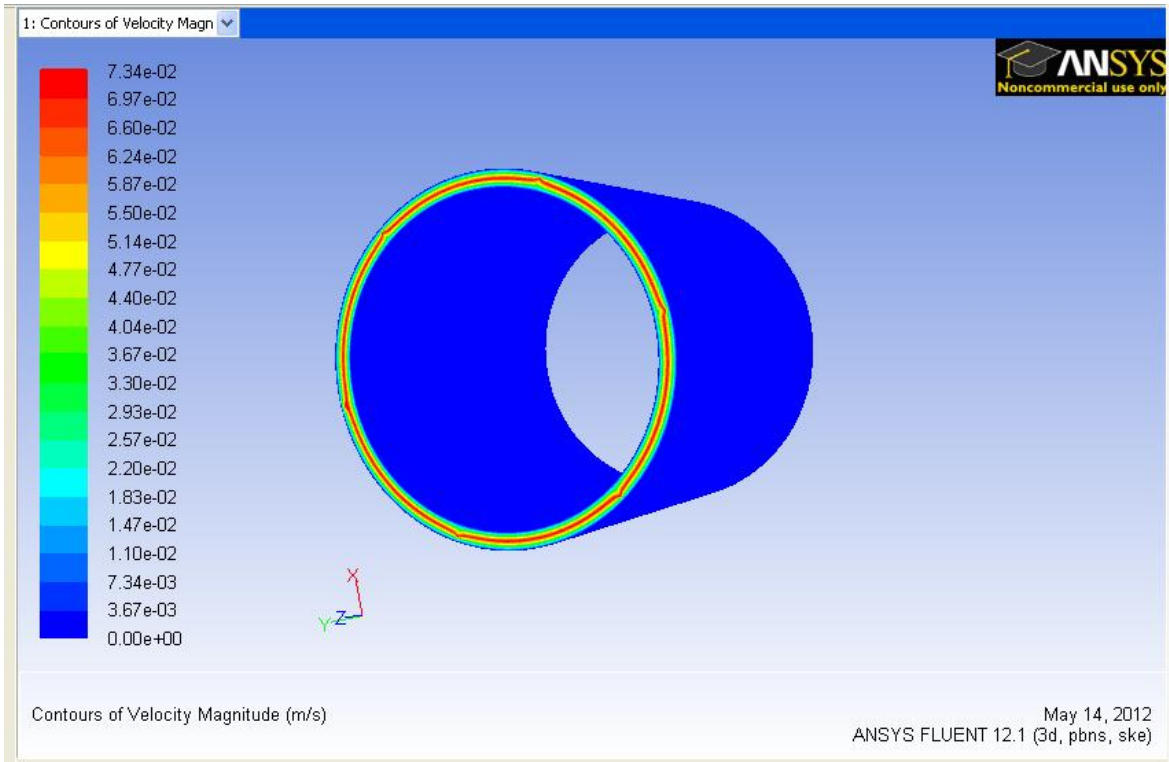
1: Contours of Velocity Magn
7.34e-02
6.97e-02
6.60e-02
6.24e-02
5.87e-02
5.50e-02
5.14e-02
4.77e-02
4.40e-02
4.04e-02
3.67e-02
3.30e-02
2.93e-02
2.57e-02
2.20e-02
1.83e-02
1.47e-02
1.10e-02
7.34e-03
3.67e-03
0.00e+00
ANSYS
Noncommercial use only
Contours of Velocity Magnitude (m/s)
May 14, 2012
ANSYS FLUENT 12.1 (3d, pbns, ske)

Vita

Mr. Jesus Nunez Michel is a researcher at the Center of Space Exploration and Technology Research cSERT (Combustion and Propulsion Lab) located at the University of Texas at El Paso. He received his Bachelors of Science in Mechanical Engineering at the University of Texas at El Paso in the Spring of 2010

Permanent address: 1458 Jim Larabel

El Paso, Texas, 79936

This thesis/dissertation was typed by Jesus Nunez